

Deliverable D11.5: Final report on the validity assessment of vertical absorption coefficient and SSA profiles by remote sensing, with Preparation of Standard Operating Procedures

Alexandra Tsekeri¹, Vassilis Amiridis¹, Anton Lopatin², Eleni Marinou^{1,3}, Eleni Giannakaki^{4,5}, Michael Pikridas⁶, Jean Sciare⁶, Eleni Liakakou⁷, Evangelos Gerasopoulos⁷, Sebastian Duesing⁸, Joel C. Corbin⁹, Robin L. Modini⁹, Martin Gysel-Beer⁹, Nicolas Bukowiecki⁹, Holger Baars⁸, Ronny Engelmann⁸, Birgit Wehner⁸, Michael Kottas¹, Panagiotis Kokkalis¹, Panagiotis I. Raptis⁷, Iasonas Stavroulas⁶, Christos Keleshis⁶, Detlef Müller¹⁰, Stavros Solomos¹, Ioannis Biniatoglou¹¹, Dimitra Konsta¹, Nikolaos Mihalopoulos⁷, Alexandros Papayannis¹², Iwona S. Stachlewska¹³, Kostas Eleftheriadis¹⁴, Prodromos Fetfatzis¹⁴, Julia Igloffstein⁸, Ulla Wandinger⁸, Albert Ansmann⁸, Oleg Dubovik², Philippe Goloub², Alberto Cazorla^{15,16}, Juan Andrés Casquero-Vera^{15,16}, Roberto Román^{15,16}, Carlos Toledano¹⁷, Andrés Alastuey¹⁸, Gloria Titos¹⁸, Noemi Pérez¹⁸, Gregori de Arruda Moreira^{15,16}, Juan Luís Guerrero-Rascado^{15,16}, Pablo Ortiz-Amezcu^{15,16}, Christine Böckmann¹⁹, Daniel Pérez-Ramírez^{15,16}, Maria Rita Perrone²⁰, Grisa Močnik^{21,22}, Inmaculada Foyo-Moreno^{15,16}, José Antonio Benavent-Oltra^{15,16}, Andrés Bedoya^{15,16}, Hassan Lyamani^{15,16}, Francisco José Olmo^{15,16}, Lucas Alados-Arboledas^{15,16}

¹ *Institute for Astronomy Astrophysics Space Applications and Remote Sensing, National Observatory of Athens, Athens, Greece*

² *Laboratoire d'Optique Atmosphérique, Université de Lille, Lille, France*

³ *Laboratory of Atmospheric Physics, Department of Physics, Aristotle University of Thessaloniki, Thessaloniki, Greece*

⁴ *Finnish Meteorological Institute, Kuopio, Finland*

⁵ *Department of Environmental Physics and Meteorology, Faculty of Physics, University of Athens, Athens, Greece*

⁶ *The Cyprus Institute, Environment Energy and Water Research Center, Nicosia, Cyprus*

⁷ *Institute for Environmental Research and Sustainable Development, National Observatory of Athens, Athens, Greece*

⁸ *Leibniz Institute for Tropospheric Research, Leipzig, Germany*

⁹ *Laboratory of Atmospheric Chemistry, Paul Scherrer Institute, Villigen, Switzerland*

¹⁰ *School of Physics, Astronomy and Mathematics, University of Hertfordshire, Hatfield, UK*

¹¹ *National Institute of R&D for Optoelectronics, Magurele, Ilfov, Romania*

¹² *Physics Department, National Technical University of Athens, Athens, Greece*

¹³ *Institute of Geophysics, Faculty of Physics, University of Warsaw, Warsaw, Poland*

¹⁴N.C.S.R. "DEMOKRITOS", Athens, Greece

¹⁵Andalusian Institute for Earth System Research (IISTA-CEAMA), Granada, Spain

¹⁶Department of Applied Physics, University of Granada, Spain

¹⁷Atmospheric Optics Group (GOA), University of Valladolid (Spain)

¹⁸Institute of Environmental Assessment and Water Research (IDAEA), CSIC, Barcelona, Spain

¹⁹Institute of Mathematics, Potsdam University, Potsdam, Germany

²⁰DipartimentodiMatematica e Fisica, UniversitàdelSalento, Lecce (Italy)

²¹Aerosol d.o.o. Research and Development Department, Ljubljana, Slovenia

²²Department of Condensed Matter, Jozef Stefan Institute, Ljubljana, Slovenia

Work package no	WP11 Improving the accuracy of aerosol light absorption determinations
Deliverable no.	D11.5 Final report on the validity assessment of vertical absorption coefficient and SSA profiles by remote sensing, with Preparation of Standard Operating Procedures
Lead beneficiary	NOA
Deliverable type	<input checked="" type="checkbox"/> R (Document, report) <input type="checkbox"/> DEC (Websites, patent fillings, videos, etc.) <input type="checkbox"/> OTHER: please specify
Dissemination level	<input checked="" type="checkbox"/> PU (public) <input type="checkbox"/> CO (confidential, only for members of the Consortium, incl Commission)
Estimated delivery date	Month 46
Actual delivery date	28/02/2019
Version	
Comments	

1 INTRODUCTION

The novel remote sensing and in situ instrumentation included in the ACTRIS research infrastructure, offers a unique opportunity for a comprehensive absorption characterization of anthropogenic and natural aerosols, within urban and remote sites of the network in Europe. JRA1 is a joint research activity of ACTRIS-2 focusing on reducing the uncertainty in the determination of the aerosol light absorption vertical profiles by combining and optimizing advanced remote sensing and in situ methods. The motivation, goals and activities for JRA1 are summarized in Fig. 1: The vertical distribution of the absorption coefficient and the SSA were retrieved via surface and airborne in situ measurements and remote sensing techniques, and dedicated ACTRIS-2 JRA1 campaigns were organized to perform closure studies between these different methods.

More specifically, the goal was to integrate the in-situ techniques employed in JRA1 Task11.1 for measuring the aerosol absorption properties with the corresponding remote sensing retrievals developed in Task 11.2 (i.e., lidar stand-alone and GARRLiC/GRASP algorithms), in order to assess their uncertainties and finally produce a representative aerosol absorption model for climate studies. For this purpose, the ACTRIS-2 JRA1 campaigns were organized during the project, employing remote sensing instruments together with in-situ absorption instruments on UAVs, tethered balloons and the ACTOS helicopter platform. Specifically, the Task 11.3 campaigns were held in Melpitz, Germany (May-June 2015 and January-March 2017), in Athens, Greece (December 2015 – February 2016), in Nicosia/Agia Marina/Orounda, Cyprus (May-June 2016 and April 2017), in Granada in Spain (May-September 2016 and May-October 2017) and in Finokalia in Crete, Greece (April 2017). The Agia Marina Xyliatou campaign was not part of the original proposal, but it was included later as a joint activity with the FP7-BACCHUS project campaign (impact of Biogenic versus Anthropogenic emissions on Clouds and Climate: towards a Holistic UnderStanding) organized in Cyprus. The in situ/remote sensing absorption profiling comparisons are provided herein only for the campaigns analyzed so far, i.e., the first JRA1 campaign in Melpitz on 2015, the Athens campaign, the Nicosia/Agia Marina/Orounda, Cyprus campaigns and the Granada campaign (SLOPE).

The **standard operation procedures** followed to derive the in situ and remote sensing absorption profiles and perform their comparison is provided in Section 2. The progress achieved in the framework of each of the aforementioned campaigns is presented in Section 3. The conclusions are discussed in Section 4.

WP11: Improving the accuracy of aerosol light absorption determinations (JRA1)

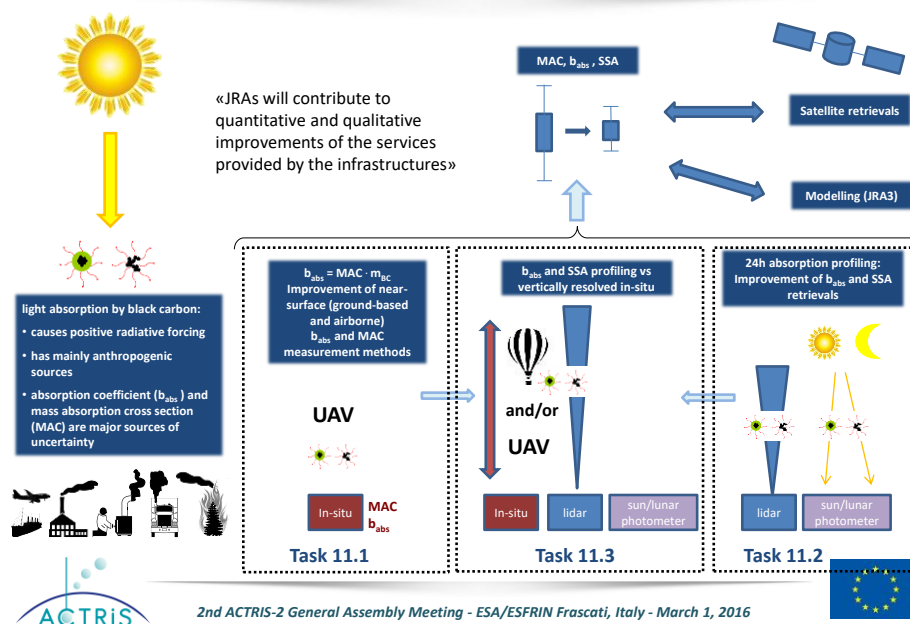


Figure 1: The motivations, goals and activities of JRA1.

2 STANDARD OPERATION PROCEDURES

2.1 In situ absorption profile measurements

Aerosol absorption can be measured with in situ measurements in real time using optical methods. The miniaturized absorption instruments deployed on Unmanned Aerial Vehicles (UAVs) during the JRA1 campaigns utilize an aerosol sample-laden filter area where light is transmitted through and the particle absorption is calculated from the light attenuation. The miniaturized absorption instruments used are 1) a single wavelength commercially available absorption monitor (Magee Scientific - Model AE51), 2) a dual wavelength prototype monitor that was custom made from the AE51 model and 3) a tricolor absorption photometer prototype (Brechtel Inc - Model 9400), referred herein as AE51, DWP and STAP respectively (see Table 1 and Fig. 2). Their performance is presented in D11.1 ([http://www.actris.eu/Documentation/ACTRIS2IAinH2020\(20152019\)/Deliverables.aspx](http://www.actris.eu/Documentation/ACTRIS2IAinH2020(20152019)/Deliverables.aspx)) and is briefly described here.

A different approach was followed by the Aerodyne CAPS-PM_{ssa} monitor onboard the ACTOS airborne platform during the Melpitz 2015 campaign, which provides the particle absorption by measuring the extinction and scattering of the light. The Aerodyne CAPS-PM_{ssa} monitor has been developed with the goal of providing accurate in-situ SSA measurements. Its performance during the Melpitz 2015 campaign is presented in Corbin et al. (2016) and is briefly discussed here.

Table 1. Characteristics of the miniaturized absorption instruments. (Source: D11.1)

Instrument Name	Flowrate (Lpm)	Spot Area (m ²)	Wavelengths (nm)	Face Velocity (m s ⁻¹)
AE51	0.1-0.2	7.1×10 ⁻⁶	880	0.5
DWP	2	7.1×10 ⁻⁶	370, 880	4.7
STAP	1.3	17.7×10 ⁻⁶	445, 515, 633	1.2

Miniaturized absorption instruments

The miniaturized aethalometers measure the particle absorption using an aerosol sample-laden filter area where light is transmitted through, while light is simultaneously transmitted via an aerosol-free (unloaded) filter spot (reference signal). The particle absorption coefficient is then calculated correcting for the multiple scattering induced by the filter fibers, using the multiple scattering optical enhancement factor (C), as well as for the loading (see more details in D11.1). For the AE31 a range of values have been proposed but 3.5 is recommended by the ACTRIS network. The loading correction depends on aerosol characteristics such as composition and size, and has to be calculated at each instance. Several empirical corrections have been suggested (Weingartner et al., 2003; Virkkula et al., 2005; Virkkula, 2010) based on commercially available instruments (e.g. Magee Scientific Model A31; Radiance Research - PSAP) at which the filter changes automatically. However, the filter strip of the miniaturized instruments examined in Task 11.1 is manually changed prohibiting the use of some of the proposed empirical corrections. In this work the loading corrections are assumed to be equal to unity provided that the attenuation of each filter does not exceed 20%, as suggested by Ferrero et al. (2011).

The AE51 is the lightest instrument which is a major asset for UAV observations. On the other hand, it may lack sensitivity for low concentrations of absorbing material which is an issue when investigating the atmospheric column and low concentrations of aerosols usually met in the troposphere. DWP and STAP have a higher flowrate (and face velocity) which may improve sensitivity for low concentrations. They have also the potential to derive information regarding absorbing material other than black carbon (Sandradewi et al., 2008). On the other hand they are heavier (≈ 1 kg) which may represent a major constraint for UAV flights (autonomy and capacity to reach high altitudes).

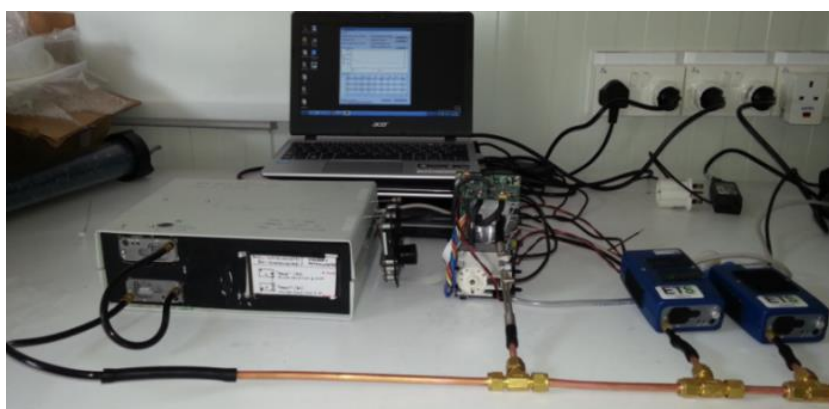


Figure 2: Ambient intercomparison for miniaturized absorption monitors. From left to right: DWP, STAP and two AE51. (Source: D11.1)

During the Athens JRA1 campaign the performance of AE51, DWP and STAP, was investigated under realistic flying conditions on board a UAV, on the ground against commercially available instrumentation (AE33 and MAAP) and under controlled conditions. All instruments were used as provided by the manufacturer without any modifications. A summary of the intercomparison results is shown in Table 2 with respect to the absorption coefficient. All examined monitors underestimated absorption when subjected to BC concentrations exceeding $15 \mu\text{g m}^{-3}$. The precision of DWP and AE51 was found to deteriorate below a certain concentration threshold, different for each of the two instrument and shown in Table 2, while STAP performed equally well under the entire range below $10 \mu\text{g m}^{-3}$. Even though STAP provided the least accurate results, the difference among the other two monitors examined was marginal.

Table 2. Comparison summary between miniaturized absorption monitors and AE33 based on the “MAAP reference” scenario (described in D11.1). Both precision and accuracy results are shown.
(Source: D11.1)

Instrument	Overall Accuracy at 370 nm	Overall Accuracy at 880 nm	Absorption Threshold (Mm ⁻¹)	Median 1-min std* below the threshold (Mm ⁻¹)	Maximum observed 1-min std* below the threshold (Mm ⁻¹)	Median 1-min std* above the threshold (Mm ⁻¹)
AE51	N/A	0.74±0.068	7	8	40	8
DWP	0.49±0.08	0.61±0.095	3.5	1.5	10	1
STAP	0.43±0.03	0.60±0.047	N/A	2.6	N/A	2.6

* standard deviation

Aerodyne CAPS-PM_{ss}a monitor

The uncertainty of the filter response for the miniaturized absorption instruments presented above, resulting in the empirical C value correction, can impart significantly the uncertainty to the reported aerosol absorption coefficient and SSA (Collaud-Coen et al., 2010). The Aerodyne CAPS-PM_{ss}a monitor has been developed with the goal of providing accurate in-situ SSA measurements. The instrument measures the reduced path length of light in an optical cavity by monitoring the phase shift of a modulated LED signal (the “CAPS” technique, Kebejian et al., 2007). In the CAPS-PM_{ss}a, an integrating-sphere nephelometer simultaneously measures scattered light exiting the same optical cavity (Onasch et al., 2015). Thus scattering and extinction coefficients are measured on the same volume; scattering is calibrated against extinction to reduce measurement bias.

Corbin et al. (2016) evaluated the CAPS-PM_{ss}a against standard optical measurements – MAAP and nephelometer, with aethalometer-derived wavelength dependence, during the JRA1 campaign in Melpitz, 2015. The site was characterized by a high SSA, negligible brown carbon absorption, and relatively low aerosol loadings. They concluded that the CAPS-PM_{ss}a approach provides sufficiently accurate measurements of SSA, even when SSA is ~0.9 and the absorption coefficient is below 50 Mm⁻¹ at 630 nm. However, its extinction measurements must be validated, and wavelength dependence is better measured by a single multi-wavelength instrument. Furthermore, the truncation of the scattering signal was found to be greater than reported in the original literature (see Fig. 5 in D11.4), which needs to be corrected for when retrieving the absorption coefficient of high SSA aerosol.

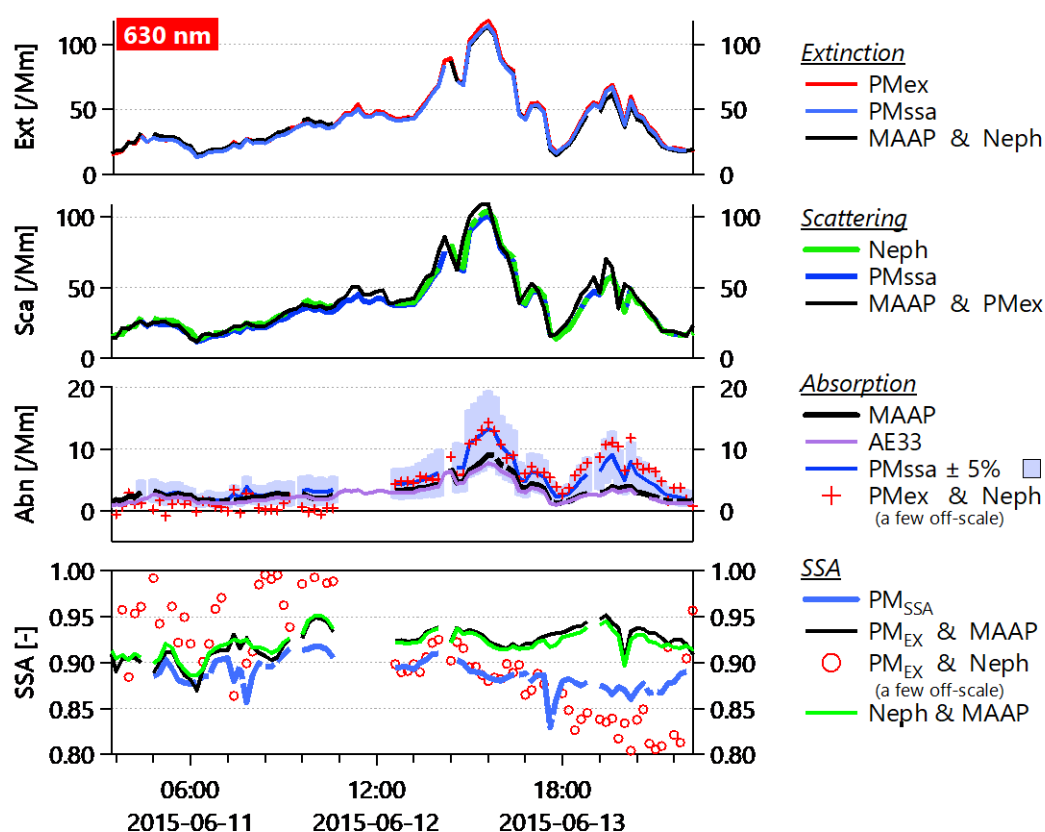


Figure 3: Time-series extract from the Melpitz 2015 JRA1 campaign, for measurements at 630 nm only. Blue shading represents the estimated calibration uncertainty of the CAPS-PMssa. The break in the data at 12:00 is due to a nephelometer calibration. (Source: Corbin et al., 2016)

2.2 Remote sensing absorption profile retrievals

The remote sensing retrieval of the absorption vertical structure is performed with the synergy of passive and active remote sensing instruments, i.e. multiwavelength lidars and sun-photometers. The sun-photometer provides the columnar properties of the particles (e.g. Dubovik and King, 2000), whereas lidars are capable of providing vertically-resolved profiles of the backscatter and extinction coefficients, along with vertical profiles of the particle microphysical properties, mainly for the fine mode (e.g. Müller et al., 2001). The Generalized Aerosol Retrieval from Radiometer and Lidar Combined data algorithm (GARRLiC/GRASP–Lopatin et al. 2013), developed in the framework of ACTRIS, goes a step further using for the first time both sun-photometer and lidar measurements in the combined retrieval of the particle microphysical properties.

More specifically, GARRLiC/GRASP algorithm utilizes the sun-photometer sun and sky measurements at four wavelengths (at 440, 670, 870 and 1020 nm) and up to 35 scattering angles, together with the vertically-resolved lidar measurements of the elastic backscatter at three wavelengths (at 355, 532, and 1064 nm). The algorithm calculates the size distribution, spherical particle fraction and spectral complex refractive index, separately for fine and coarse particles, considering them constant along the atmospheric column, as well as the volume concentration profiles of fine and coarse particles. Figure 4 shows the algorithm's input and output. The volume concentration below the lowest height of the lidar signals is considered to be constant. Moreover, in case of a dominant mode (e.g. pure dust cases), the algorithm is set to retrieve the aerosol characteristics for one mode only.

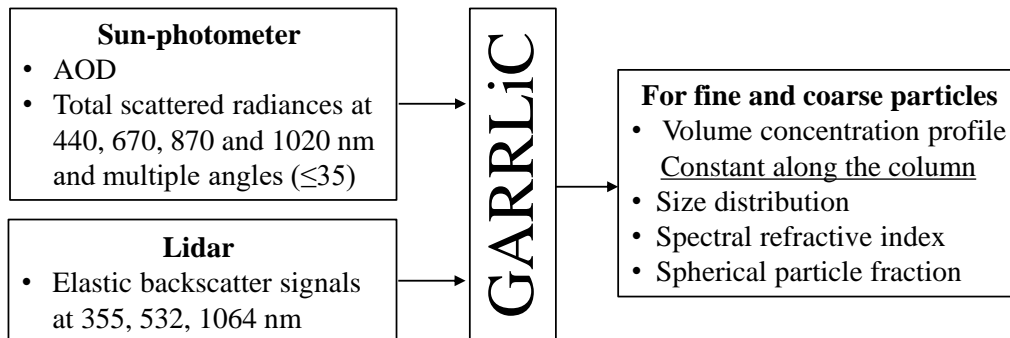


Figure 4: The GARRLiC/GRASP algorithm input and output parameters.

During the ACTRIS-2 JRA1 campaigns, intensive ground-based active and passive remote sensing measurements were performed with PollyXT and MULHACEN lidars and CIMEL sun-photometers. Both GARRLiC/GRASP and the lidar stand-alone algorithms of Müller et al. (2001) and Boeckman (2001) are used to produce the absorption coefficient and SSA vertical profiles.

3 IN SITU AND REMOTE SENSING ABSORPTION PROFILE COMPARISONS

3.1 MELPITZ CAMPAIGN (2015)

From May 4 until July 10 2015 the Melpitz column campaign was performed at the ACTRIS site Melpitz (Germany), 40 km north east of Leipzig. The campaign was led by TROPOS with contributions from PSI, Universities of Bayreuth, Braunschweig, Darmstadt, and Tübingen as well as from the German Weather Service (DWD). The main goal of the campaign was the detailed characterization of the column above the Melpitz site in terms of aerosol particles, their radiative properties and meteorological parameters. Surface in-situ measurements of Black carbon (BC) showed daily averages below $0.5 \mu\text{g m}^{-3}$ in the fraction below $1 \mu\text{m}$ during the whole campaign and below $0.25 \mu\text{g m}^{-3}$ during the intensive period with airborne measurements. These values are very low and characterize a very clean period. The aerosol optical depth (AOD) at 500 nm measured in Melpitz was always below 0.3 during the intensive period.



Figure 5: Schematic of the Melpitz column: Combination of ground-based in-situ, ground-based remote sensing and airborne measurements of aerosol particles and their optical properties.

Instrumentation

During the campaign a number of ground based instruments was operated in Melpitz (Spindler et al., 2013) continuously measuring basic meteorology, chemical composition of PM₁, ionic inorganic aerosol constituents and gases, trace gases, particle mass concentration of PM₁₀, PM_{2.5} and PM₁, particle number size distribution (ambient and non-volatile), particle absorption, extinction and scattering. In addition, a number of ground based remote sensing systems was deployed for that period: multiwavelength-Raman lidar, lunar/ sun photometer, Doppler lidar, microwave radiometer, cloud radar, and ceilometer.

During intensive periods, mainly between June 15 and July 2, additional airborne measurements were performed using the helicopter-borne platform ACTOS (Siebert et al., 2006), a tethered balloon, the UAV ALADINA (Altstädter et al., 2014) and MASC (Wildmann et al., 2014) as well as a research aircraft. Their instrumentation was focused on aerosol particles, turbulence and optical parameters. The in situ measurements of the absorption coefficient and the SSA presented here was realized by using the helicopter-borne platform ACTOS equipped with instrumentation to measure optical properties under dry conditions (< 40% RH) such as aerosol absorption coefficient at 3 wavelengths (STAP, Brechtel Inc., 450, 525, 624 nm) and aerosol extinction at 1 wavelength (CAPS- PM_{ssa}, Aerodyne Inc., 630 nm). The helicopter performed 12 measurement flights with a maximum duration of 2 h each.

The remote sensing retrievals of the absorption profiles were derived using measurements from the automated PollyXT Oceanet lidar (Engelmann et al., 2016), measuring continuously profiles of particle backscatter coefficients at 355, 532 and 1064 nm, particle extinction coefficients at 355 and 532 nm (nighttime and early morning/late afternoon only) and particle depolarization ratio under ambient conditions, as well as the lunar/sun photometer, measuring direct and diffused sunlight at different wavelengths between 340 and 1640 nm. From the combination of sun photometer and lidar, one can obtain microphysical properties and advanced optical parameters like the particle absorption coefficient

and SSA from lidar stand-alone and GARRLiC/GRASP algorithms, as discussed in Section 2. However, all retrievals have their limitations: GARRLiC/GRASP and the lidar stand-alone algorithms usually need sufficient AOD to retrieve reliable results. On top of this, the lidar stand-alone inversion relies on the Raman signals which are available at night time only.

Absorption profiles on 24/6/2015

On 24 June 2015 a steady layer extending from the surface up to ~ 2 km is shown in the lidar measurements. The only available time for a combined lidar/sun-photometer retrieval is at 18:00-19:20 UTC due to low clouds before and after that time (Fig. 8). We performed a GARRLiC/GRASP retrieval using the lidar measurements at this interval and the sun-photometer measurements at 17:50 UTC. The in situ measurements performed with STAP and CAPS-PMssa instruments onboard the ACTOS platform were acquired earlier in the day, at 13:45-15:48 UTC (Fig. 8), when we cannot use GARRLiC/GRASP due to the low clouds present. Although the remote sensing and the in situ measurements were not collocated, we expected that the spatial and temporal differences will not be very large, due to the steady form of the aerosol layer.

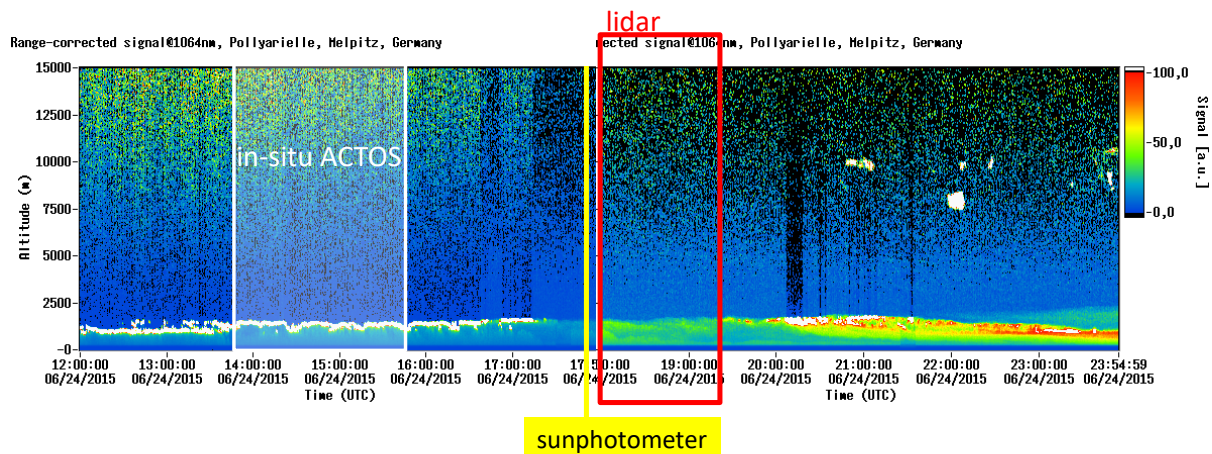


Figure 7: Lidar range-corrected backscattered signal at 1064 nm, on 24 June, 2015, during the JRA1 Melpitz campaign. The red box denotes the lidar measurements used for the absorption coefficient profile retrieval with the GARRLiC/GRASP algorithm at 18-19:20 UTC, the yellow line denotes the sun-photometer measurements at 17:50 UTC and the white box denotes the time range (13:45-15:48 UTC) of the in situ measurements acquired with the ACTOS airborne platform.

For this case the aerosol load was low, with an AOD at 440 nm of 0.14. The particles were not very absorbing (SSA at 500 nm > 0.9). These factors posed difficulties both for the GARRLiC/GRASP retrieval, as well as the in situ absorption measurements. The GARRLiC/GRASP results showed large uncertainties (~ 7 Mm^{-1}), but they had similar slopes with the in situ absorption profiles, although they produce larger values (Fig. 8 –solid lines in plots). The STAP and CAPS-PMssa absorption coefficient at 630 nm seemed to agree within the uncertainty of the measurements, although the CAPS-PMssa measurements showed slightly higher values.

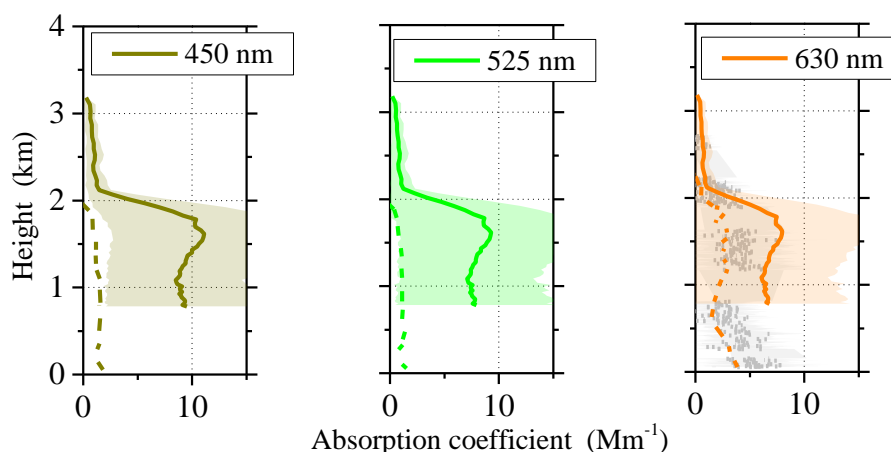


Figure 8: Absorption coefficient profiles retrieved from remote sensing measurements, from GARRLIC/GRASP algorithm (colored solid lines), and measured with airborne in situ instruments, i.e. CAPS-PMssa monitor (grey dash line) at 630 nm and STAP (colored dash lines) at 450, 525 and 624 nm, on 24 June 2015, during the JRA1 Melpitz campaign. The shading colors show the corresponding uncertainty estimates for GARRLIC retrievals and CAPS-PMssa measurements.

General remarks

Due to the low absorption coefficients during Melpitz Column 2015 a closure between airborne in situ measurements and remote sensing retrievals was not successful. The AOD (at 500 nm) was below 0.3 during all the time, so that the novel developed algorithms could not be applied to retrieve the absorption coefficient.

3.2 ATHENS CAMPAIGN

The Athens smog ACTRIS JRA1 campaign focused on the alterations of the absorption of the man-made aerosol pollution in the urban environment of Athens due to economic crisis, concentrating on the "smog" phenomenon caused by wood-burning for heating purposes. The campaign took place from 15th of December 2015 until 29th of February 2016 at the Thissio site, Athens, Greece. Specifically, the aerosol characterization was established by ground-based active/passive remote sensing techniques, surface in-situ measurements and airborne (UAV) observations. The tethered balloon in situ measurements scheduled in the proposal were not possible, due to flight restrictions at the site. A description of the campaign, along with an overview of all the acquired measurements is available at the campaign website: <http://actris-athens.eu/>

Measurements

Surface In-situ measurements

Surface measurements of optical parameters were conducted throughout the campaign. Black Carbon / absorption coefficient measurements took place by means of the Thermo 5012 Multi Angle Absorption Photometer (MAAP) and the Magee Scientific Aethalometer AE33 (AE-33). MAAP Black Carbon (BC) mass concentration values (<20 $\mu\text{g m}^{-3}$) at 670 nm were available under time resolution of 30 minutes. The 7 λ -AE33 (370, 470, 520, 590, 660, 880 and 950 nm) collected continuously aerosol sample in time base of 1 min under total flow of 5LPM. The measurement of absorption at 880 nm was interpreted as concentration of Black Carbon (BC). Elemental Carbon (EC) was also determined in the PM_{2.5} fraction of

quartz filter samples acquired over 12-hour periods (6:00-18:00 and 18:00-6:00 in order to determine the role of different processes/sources between day and night-time respectively) by a dichotomous automatic filter sampler (Dichotomous Partisol – Plus, Model 2025 Sequential Air Sampler). An Aurora1000 nephelometer equipped with a silica gel drier provided data of Scattering Coefficient at 525 nm, every 5 minutes. The station was equipped with an Aerosol Chemical Speciation Monitor (ACSM; Aerodyne Inc.) measuring aerosol mass and chemical composition (ammonium, sulfate, nitrate, chloride and organics) of non-refractory submicron aerosol particles in real-time and temporal resolution of 30 minutes. Total particle number size distributions in the diameter range of 10 to 487 nm were obtained every 5 minutes by a Scanning Mobility Particle Sizer (SMPS; TSI Model 3034) operating with a sheath-to-aerosol flow ratio of 4:1 liters per minute.

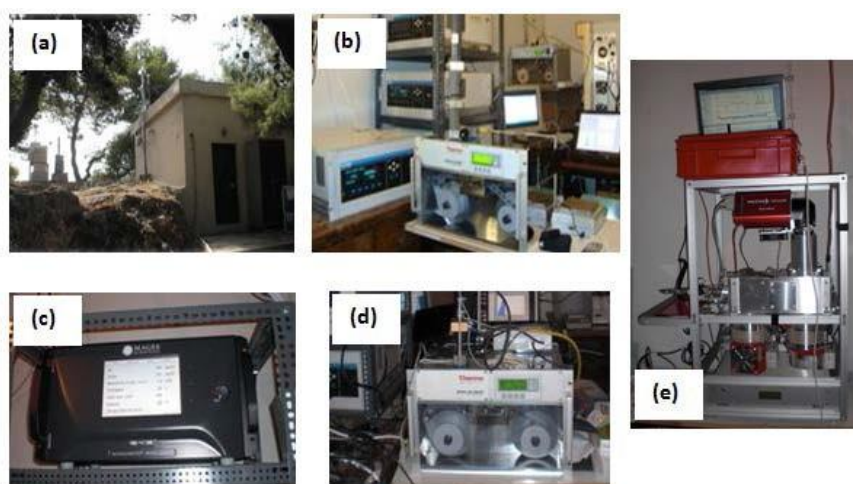


Figure 9. (a) Thissio site, (b) internal aspect, (c) AE-33, (d) MAAP and (e) ACSM apparatus during the ACTRIS-2 JRA1 Athens campaign.

Auxiliary measurements at Thissio site were also available. Aerosol mass concentration was determined based on PM_{2.5} and PM_{2.5-10} (PM₁₀ as the sum of the fine and coarse fraction) filter samples collection on 12 hours intervals. The filter samples were analyzed for the determination of ions, metals and elemental / organic carbon. Near real-time systems for monitoring of ionic and major acidic compounds (PILS-IC and WAD-IC respectively) and organic compounds (GC-FID for C₂-C₆ NMHCs) were also available. Air quality monitoring included also measurements of ozone (O₃), nitrogen oxides (NO and NO₂) and carbon monoxide (CO) using HORIBA air pollution monitoring systems (AP-360 series) and PM₁₀ (Eberline FH 62 I-R Beta-attenuation analyzer) as well. Meteorological and actionmetric parameters were provided by the IERSD/NOA automatic station.

Airborne In-situ measurements

The Cyprus Institute (Cyl) and NOA performed UAV flights for the Athens smog ACTRIS JRA1 campaign.



Figure 10. Cyl UAV with the miniaturized instrumentation.

NOA managed to get UAV flight authorization above Thissio site from the Greek Civil Aviation Authorities (CAA) with flight permission for UAV below 8kg, flight only during daytime (07:00-17:30) and at a maximum altitude of 1,000 m above ground level. It is somewhat unique to get such permission above a large urban area. NOA also managed to grant authorization from the archeological department for the UAV ground operations (take-off/landing) in a public archeological site, directly opposite to the Acropolis. Despite flight authorization, we could not investigate exhaustively the strong domestic wood burning (which happens at night) and hardly fly above the boundary layer. The Cyl had to reconsider its UAV flight strategy; purchasing a new rotary wing multi-copter (Fig. 11) (instead of using its fixed wings models) to take-off and land vertically over a small (10mx10m) area, test this new UAV (in terms of payload, autonomy, autopilot communication, aerosol instrumentation interference) and adapt specific features (aerosol sampling inlet and dryers) within a period of only 3 months prior to field deployment. Because of a total weight limitation (8kg) granted by CAA, Cyl could only fly absorption monitors (and not aerosol number concentration counters). UAV flight operation requested 4 staff members (1 accredited UAV pilot, 1 electronic engineer, 2 researchers for running/processing atmospheric sensors).



Figure 11. Picture of the Cyl rotary wing UAV equipped with Absorption sensors, T/RH/P probes and video. Photo taken from Thissio.

The performance of three miniaturized instruments, named AE51, DWP and STAP (Fig. 12), was investigated using first validation from ground-based instrumentation (MAAP, AE33). They were also evaluated under realistic UAV flying conditions. Their evaluation is briefly discussed in Section 2, with a more complete analysis provided in D11.1.



Figure 12. Pictures of the 3 miniaturized absorption instruments tested onboard the Cyl UAV. From left to right: STAP (from Brechtel), DWP (dual-wavelength prototype by Aerosol doo), and AE51 (by Aethlabs).

All of the monitors used during the campaign, involved the same principle of operation, which suffered from artifacts from humidity or temperature gradients. Therefore, the sampled air was dried, using a custom-made diffusion dryer, which however limited UAV payload further. The flight strategy was elaborated to include two early morning flights half to one hour away from each other starting at sunrise (05:00 UTC) to investigate the stratification of the atmosphere (boundary layer, low free troposphere), two late afternoon flights ending approximately at sunset (16:00 UTC) to investigate the vertical mixing of urban emissions in the atmospheric column.

NOA performed UAV flights as well, for vertical profile measurements of Black Carbon / Absorption coefficient in the atmosphere at 880 nm under 1s and/or 10s time resolution. The microAeth model AE51 was integrated onto a 6-rotor Unmanned Aerial Vehicle (UAV Hexacopter) with a diagonal wheelbase of 550 mm and an All Up Weight (AUW) of approximately 2.5 kg. The UAV is GPS flight enabled and equipped with multiple redundancies and fail-safe RTH (Return To Home) functions. It delivered a hovering accuracy of ± 0.5 m in the Vertical and ± 1 m in the Horizontal axis and maximum Ascent and Descent speeds of 6 m/sec and 4 m/sec respectively. Flight autonomy was about 14 minutes (in full throttle) and the maximum flight altitude was set to approximately 1.000 m above mean sea level. The profiles were mainly obtained during January 2016.



Figure 13. NOA UAV (left) and Miniature black carbon aethalometer (ETS AE51) (right), at the ACTRIS-2 JRA1 Athens smog campaign.

Moreover, a new Coarse Mode Aerosol Collector (CMAC) prototype sampling instrument was developed by NCSR "Demokritos" team and tested onboard the NOA hexacopter (Fig. 14). The aim of this instrument was to collect size resolved fractions of coarse particles at 6 impaction stages from different layers in the atmosphere and then analyze the samples in the lab. During February, 3 days of flights were conducted, and the two layers of the collection were chosen at 500-700 m and 200-300 m above sea level.



Figure 14. NOA UAV with the miniature coarse mode aerosol collector (CMAC)

Remote sensing measurements:

Intensive ground-based active and passive remote sensing measurements were performed during the Athens campaign (Fig. 15). The PollyXT NOA lidar operated in a 24/7 mode. The University of Warsaw participated in the campaign by providing and operating the NARLa receiver for near-range lidar measurements at 355 and 532 nm with the PollyXT. Moreover, AERONET CIMEL sun-photometer measurements were performed routinely. Cloud height and vertical visibility was measured by a CHM 15K ceilometer, kindly provided by the Lufft company (<http://lufft.com/en/products/optical-sensors/ceilometer-chm-15k-nimbus-835000/>).



Figure 15. PollyXT NOA lidar (left) at the Thissio site, CIMEL sunphotometer (upper-right) and Lufft Ceilometer (lower-right) during the ACTRIS-2 Athens smog campaign.

Figure 16 shows an overview of the remote sensing (i.e., lidar, sunphotometer) and surface in-situ measurements during the campaign. Increased level of Black Carbon and biomass burning contribution (%bb) was observed during night. BC is deconvolved into the fossil fuel and wood burning fractions, BC_{ff} and BC_{wb} respectively. A mean contribution of almost 25% biomass burning (%bb) to the total level of BC was observed, with maximum of more than 40% encountered during night. The combustion of fossil fuel was located both during morning and night. Overall, the AODs were relative low (0.2-0.3 at 440 nm) with

overcast weather as can be seen from the second and third plot, respectively. Both factors do not facilitate the lidar/sunphotometer retrievals. As discussed for the Melpitz case as well, an AOD of at least 0.3 at 440 nm was required for absorption retrievals from GARRLiC/GRASP. Moreover, most of the aerosol load in Athens smog cases was located below 1 km, at the lidar incomplete overlap region, which challenged further the retrieval. Despite of the relative low AODs, we analyzed one case on January 19 2016.

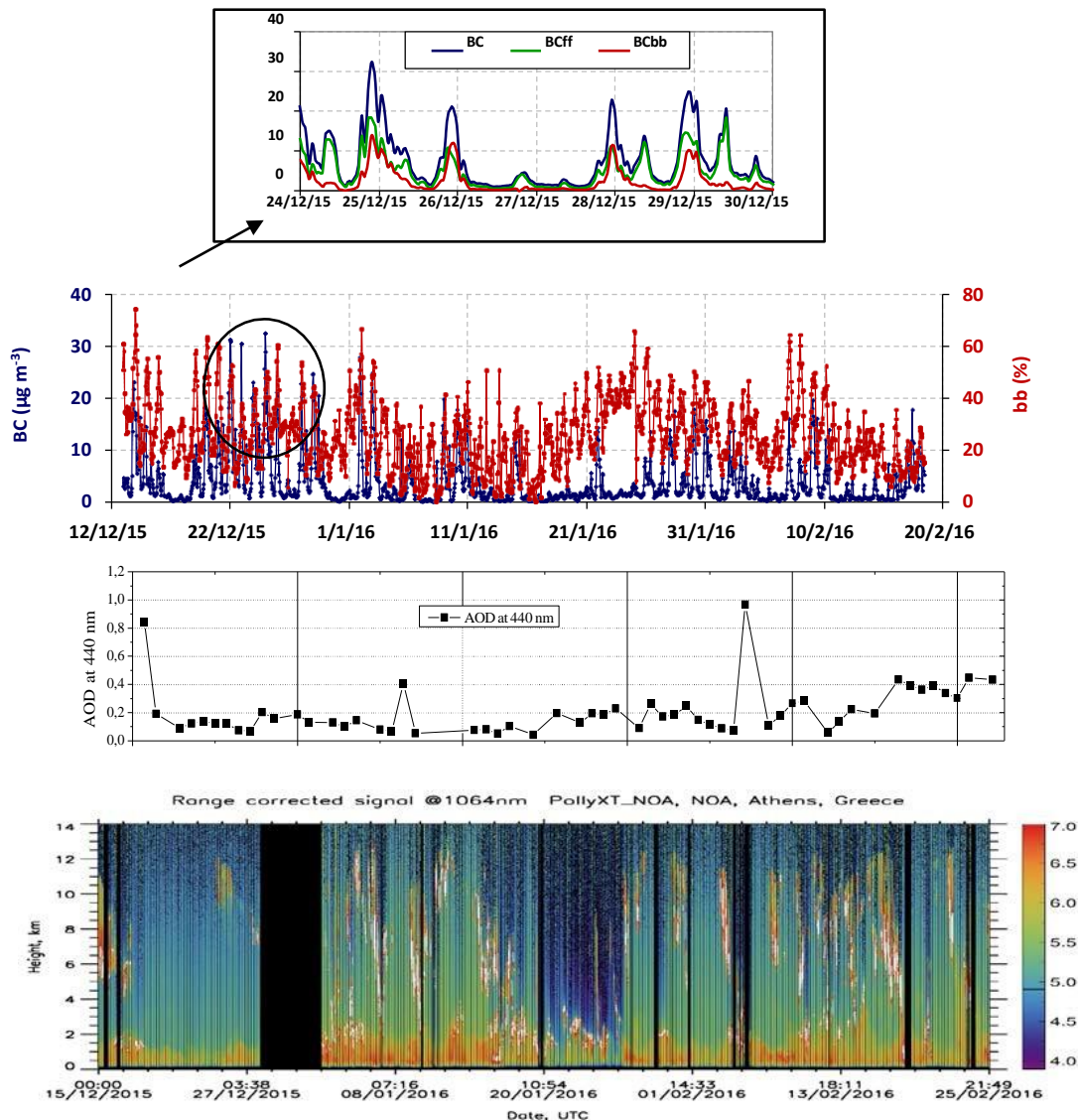


Figure 16. Surface in-situ measurements of black carbon concentration and biomass burning percentage including deconvolved fossil fuel and wood burning fractions, BCff and BCbb respectively for selected days (up), AOD at 440 nm measurements from the CIMEL sunphotometer (middle) and PollyXT NOAA 24-hour measurements (range-corrected lidar signals at 1064 nm), at the Thissio site, during the ACTRIS-2 JRA1 Athens smog campaign.

Absorption profiles on 19/1/2016

On January 19 morning PollyXT NOAA lidar measurements showed a residual aerosol plume up to ~2.5 km and a new-forming plume after 8:00 UTC, extending from the ground up to 1-2 km, indicating most probably local pollution and possibly smog (Fig. 17). The CIMEL sunphotometer measured an AOD of ~0.16 at 440 nm. During this day the UAV flights, up to 1 km a.s.l. were conducted almost every hour. The

frequency of vertical absorption profiles acquired, allowed for a reconstruction of the BC vertical distribution from 05:30 to 09:30 UTC, shown in Fig. 18 in combination with BC measurements at the ground. However, due to the cloud cover only one resulting profile (at 9:35-9:50 UTC) was compared against concurrent GARRLiC/GRASP absorption profile retrievals. The lidar data used in the GARRLiC/GRASP retrieval were acquired at 8:30-10:30 UTC, whereas the sun-photometer data were acquired later, at 11:37 UTC. This was expected to introduce uncertainties in the combined lidar/sun-photometer GARRLiC/GRASP retrieval, but unfortunately it was dictated by the non-uniformity of the lidar data after 10:30 UTC, and the formation of clouds after 11:30 UTC.

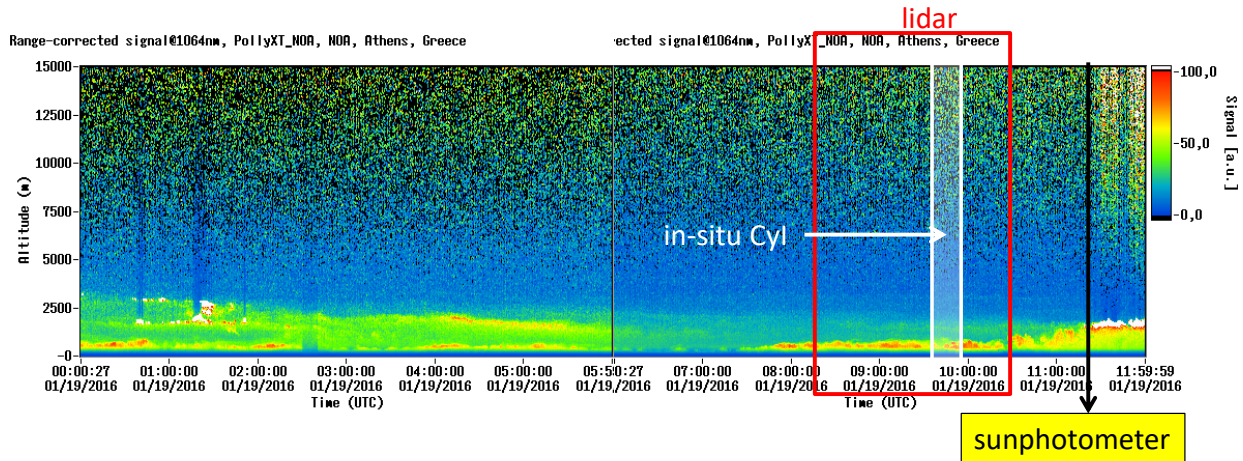


Figure 17: Lidar range-corrected backscattered signal at 1064 nm, on 19 January, 2016, during the JRA1 Athens campaign. The red box denotes the lidar measurements used for the absorption coefficient profile retrieval with the GARRLiC/GRASP at 8:30-10:30 UTC, the black line denotes the sun-photometer measurements at 11:37 UTC and the white box denotes the time range (9:35-9:50 UTC) of the in situ measurements acquired with the DWP instrument onboard the Cyl UAV.

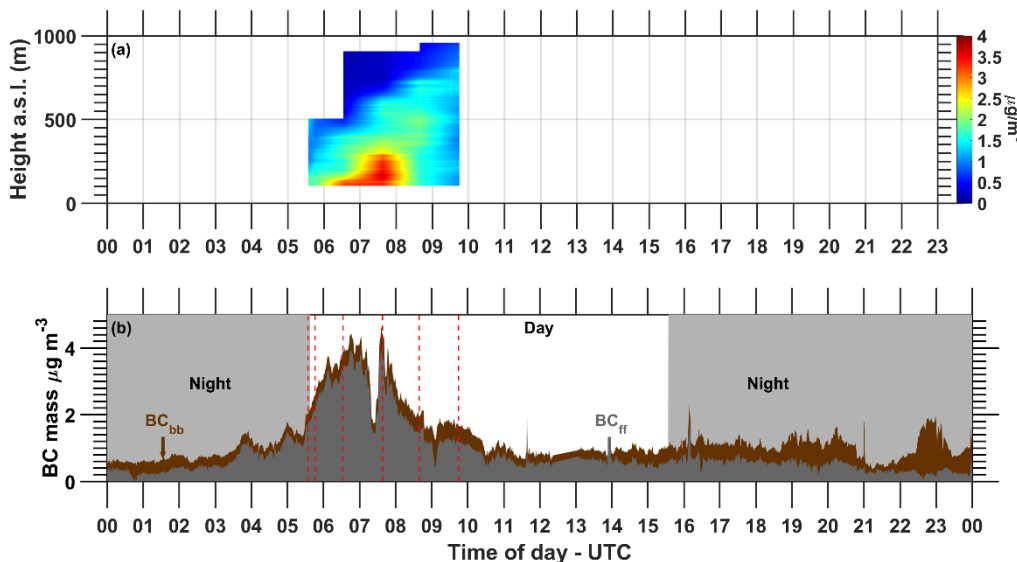


Figure 18: BC mass vertical distribution (a) based on 6 flights between 19th January 2016 05:30 and 09:30 (UTC). The corresponding ground measurements are also shown (b). The concentration of BC from fossil

fuel (ff) and biomass burning (bb) are shown with grey and brown, respectively. Dashed red lines indicate the start of each of the 6 flights the reconstructed eBC profiles was based upon.

Figure 19 shows the comparison for the absorption coefficient profiles at 880 nm from the GARRLiC/GRASP and the lidar stand-alone remote sensing retrievals, along with the in situ measurements from the DWP micro-Aethalometer on board the UAV and the surface in-situ measurements. First, we see an agreement between the GARRLiC/GRASP and the lidar stand-alone absorption coefficients, within their uncertainties. The comparison with the in situ absorption profiles does not allow clear conclusions, since the profiles do not overlap sufficiently, due to the low flight heights of the UAVs (up to 700 m a.g.l. for the case shown here). Moreover, most of the aerosol were located below ~ 1 km, in the lidar incomplete overlap region. Although the absorption values for GARRLiC/GRASP and in situ showed quantitative differences, the profile slope is similar. This is a promising finding, since the gradient of the absorption profile is very important for atmospheric stability studies.

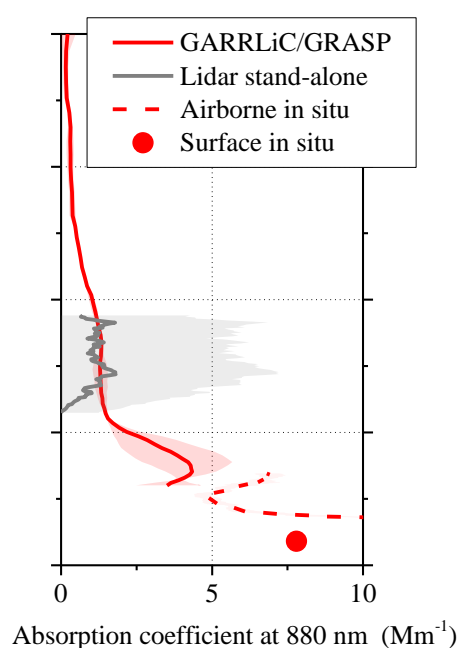


Figure 19. Absorption coefficient at 880 nm from GARRLiC/GRASP (solid colored lines) and lidar stand-alone algorithms (solid grey lines) at 8:30-10:30 UTC, along with airborne measurements (dashed red line) from the DWP micro-Aethalometer onboard the Cyl UAV at 9:35-9:50 UTC, and surface in situ measurements at 880 nm (red circle), on January 19, 2016.

3.3 CYPRUS CAMPAIGN

The mandate of the JRA1 Cyprus campaign was to investigate the influence of dust on absorption properties. The campaign was conducted in synergy with the joint FP7- BACCHUS - INUIT campaign that took place from 30 March till 28 April 2016. A suite of measurements were conducted at the Agia Marina Xyliatou (AMX) Observatory ($35^{\circ} 2'17.97''N - 33^{\circ} 3'28.50''E$, 532 m a.s.l.), on the ground and airborne at the Orounda airfield 6.74 km northerly of AMX up to a height of 2.4 km a.s.l., along with intensive ground-based active and passive remote sensing measurements conducted 33 km easterly, at Nicosia (181 a.s.l.), benefiting from the elevation difference between the AMX and Nicosia sites. The homogeneity of the

measurements between the two ground sites was validated, by the almost daily absorption vertical profiles measured at the Orounda airfield. GARRLiC/GRASP was used here for the characterization of Saharan dust and Arabian dust from the Middle East, together with possible mixtures of urban and marine particles at the Eastern Mediterranean region.

Measurements

Surface In-situ measurements

Aerosol absorption was monitored using an AE33 and a MAAP in combination with a TSI nephelometer (Model 3563) that measured total and backward scattering. Size distribution was measured a Grimm OPC (Model 1.109), a TSI APS (Model 3321) and a Pallas SMPS. Intensive measurements on the ground involved several custom-made IN monitors. The submicron chemical composition of non-refractory submicrometer particles was monitored in near-real time using an ACSM, and with a daily resolution using filters. The composition of particles with diameters below 2.5 and 10 μm was also monitored at a daily resolution.

Airborne In-situ measurements

Two types of fixed wings UAV were deployed during this 1-month campaign; Skywalker X8 and Cruiser (Fig. 20). Airborne measurements were conducted in the private airfield and private airspace (5x5km at the ground and altitude up to 3 km above sea level). This permanent private airspace was unique in the Mediterranean and was a big asset to investigate in-situ aerosol properties in the atmospheric column.



Figure 20: UAV flight operation in Cyprus with the Cyl mobile ground control station (April 2016). The black UAV is a fixed wing foam Skywalker X8.



Figure 21: Left: Medium size (4 m wing span) Cyl Cruiser UAV during flight operation. Right: Aerial view of the Cyl private runway for UAV close to the CAO station.

Remote sensing measurements

Intensive ground-based active and passive remote sensing measurements were acquired with the PollyXT NOA lidar and the CIMEL sun/lunar photometer, installed in Nicosia.

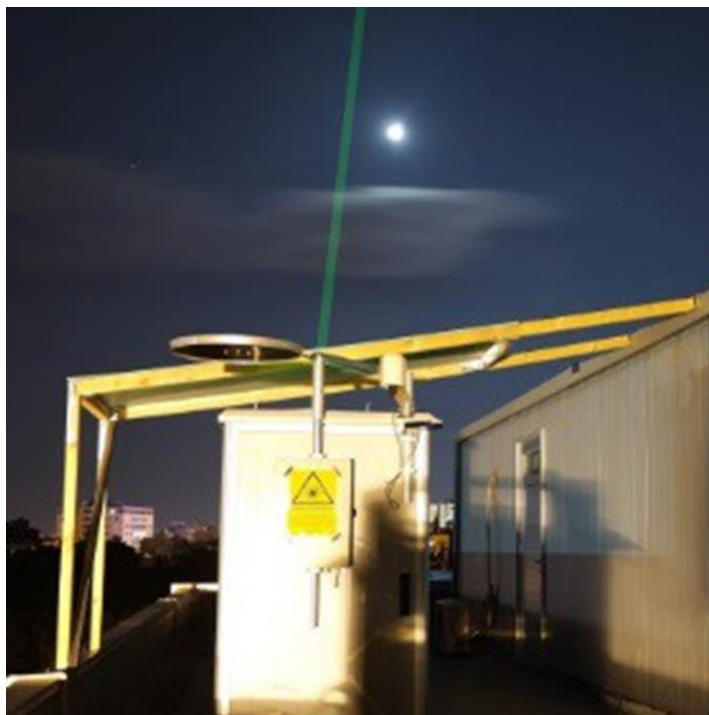


Figure 22: The PollyXT NOA lidar operating on the roof of the Cyprus Institute in Nicosia, during the JRA1 Cyprus campaign.

By contrast with observations performed in Athens which showed some gradients close to the surface, the measurements performed in Cyprus showed very homogeneous concentrations of BC in the boundary layer and close to zero values in the free troposphere as illustrated in the Fig. 23. In contrast with absorption vertical profiles, vertical gradients with respect to aerosol mass were identified, especially during periods when dust particles were transported to Cyprus (Mamali et al., 2018).

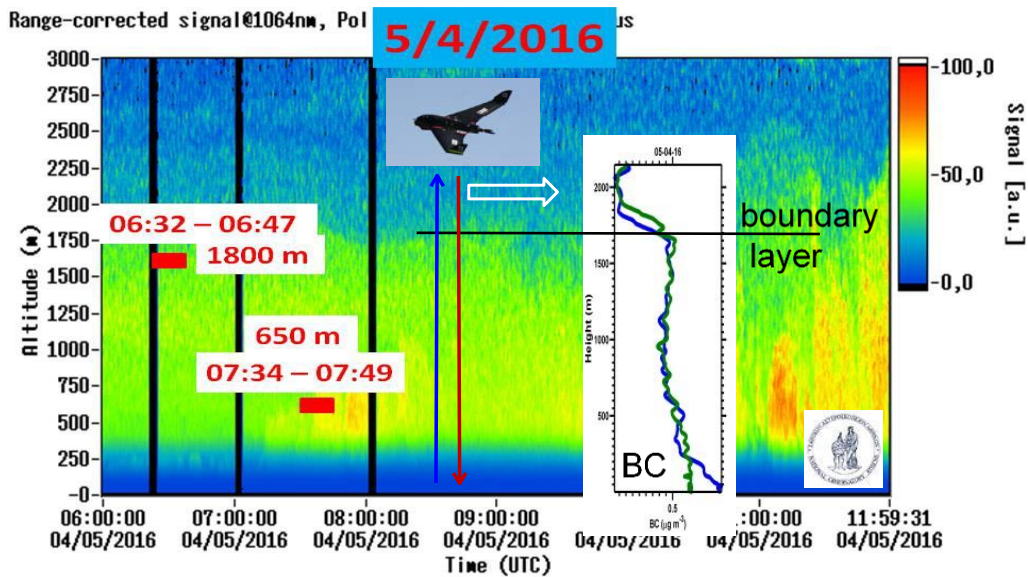


Figure 23: Illustration of 6-hour monitoring of PollyXT NOA lidar (06:00-12:00) on 4 May 2016. Red dots at 1800 m and 650 m stand for two atmospheric aerosol samples taken by UAV for off-line IN analysis. Blue and red rows at 08:30-08:45 UTC show the ascending/descending measurement of Black Carbon. Black dot line stands for the top of the boundary layer.

Absorption profiles on 7/4/2016

On 7 April 2016 the PollyXT NOA lidar measurements showed two distinct dust layers, from the surface up to ~3 km and from 3.5-7.5 km, which seemed quite stable during 00:00-12:00 UTC (Fig. 24). The lidar depolarization at 532 nm (Fig. 24) is evidence of non-spherical dust particles at the layers. The aerosol load was not very high, with AOD at 440 nm of 0.2. For the GARRLiC/GRASP absorption profile retrieval we used the lidar measurements at 4:30-6:00 UTC and the sun-photometer measurements at 5:59 UTC. The airborne in situ absorption coefficient profiles at 370 and 880 nm were acquired with the DWP aethalometer at 5:37-6:07 UTC, in good collocation with the remote sensing measurements.

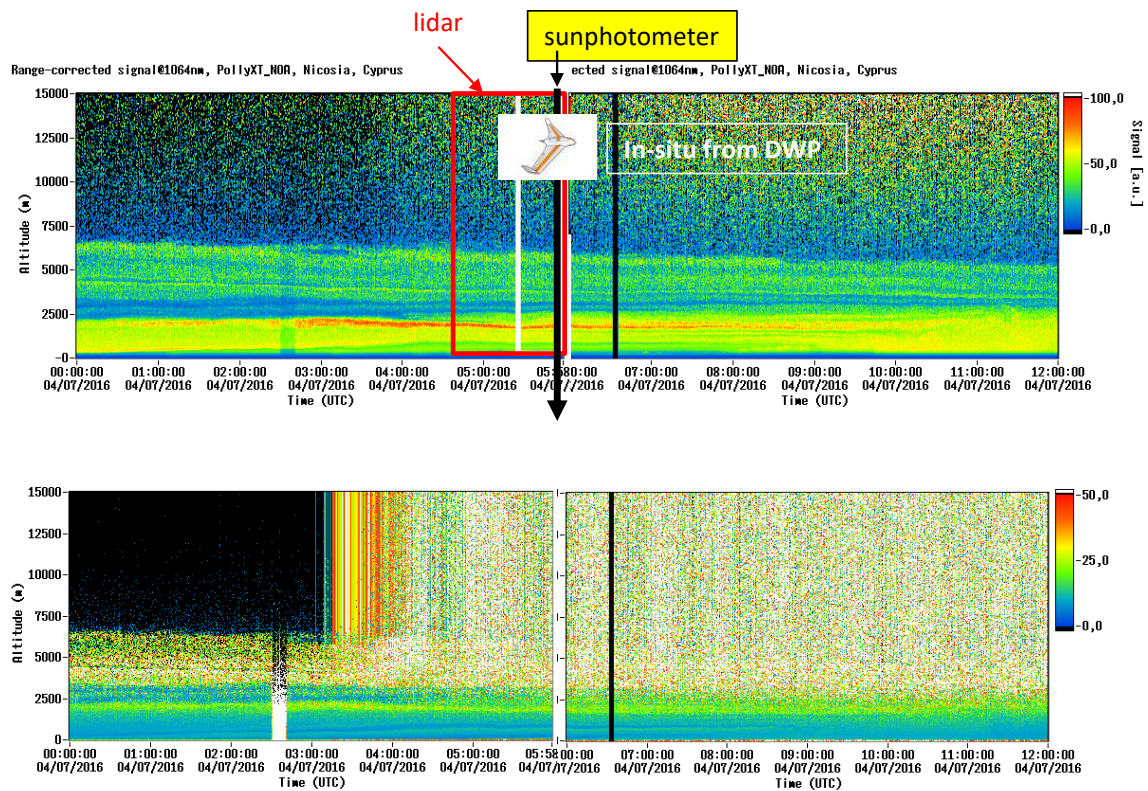


Figure 24: Top: Lidar range-corrected backscattered signal at 1064 nm, bottom: Cross/Total backscattered signal at 532 nm, on 7 April, 2016, during the JRA1 Cyprus campaign. The red box denotes the lidar measurements used for the absorption coefficient profile retrieval with the GARRLiC/GRASP algorithm at 4:30-6:00 UTC, the black line denotes the sun-photometer measurements at 5:59 UTC and the white box denotes the time range (5:37-6:07 UTC) of the in situ DWP measurements acquired with the Cyl UAV.

The comparison of the absorption coefficient profiles from GARRLiC/GRASP and the surface and airborne in situ measurements is shown in Fig. 25: the agreement was good for 370 nm, with GARRLiC/GRASP to provide smaller values for the absorption coefficient, but similar vertical structure with the airborne in situ measurements. The difference can be due to the distance between the AMX and Nicosia stations. The agreement at 880 was not so satisfactory, with GARRLiC/GRASP to provide much lower values than the airborne in situ measurements. One of the reasons for this discrepancy may be the low absorption coefficient values at 880 nm ($<10 \text{ Mm}^{-1}$), which is not optimum neither for the remote sensing retrieval, nor for the in situ measurements. The airborne and surface in situ measurements seemed to agree well at both 370 and 880 nm.

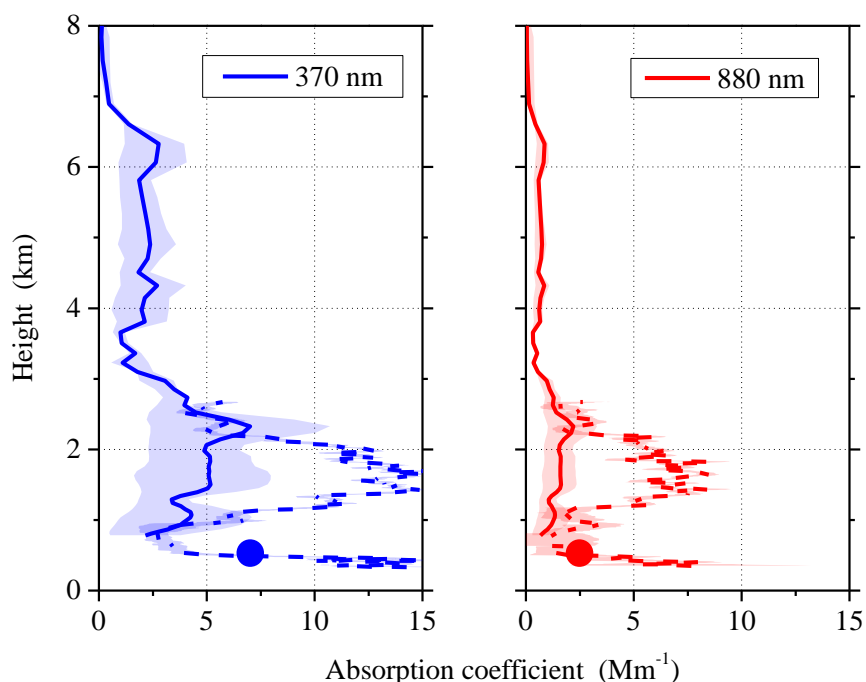


Figure 25. Absorption coefficient at 370 nm (left) and 880 nm (right) from GARRLiC/GRASP (solid colored lines) at 4:30-6:00 UTC, along with airborne measurements (dashed colored lines) from the DWP micro-Aethalometer onboard the Cyl UAV at 5:37-6:07 UTC, and surface in situ measurements (circles), on April 7, 2016.

Absorption profiles on 15/4/2016

On 15 April 2016 we recorded a moderate dust episode, with AOD at 440 nm of 0.3 (Fig. 26). The airborne in situ measurements were conducted under cloudy conditions at 9:27-9:55 UTC, during which we could not perform the GARRLiC/GRASP retrieval. Instead we used lidar and sunphotometer measurements earlier in the day (at 5:00-6:00 UTC and 5:06 UTC, respectively). The dust plume showed variations throughout the day (Fig. 26), thus the comparison of non-collocated remote sensing and in situ measurements was expected to show discrepancies between them.

Although the adequate aerosol load, the particles were not strongly absorbing, with the absorption coefficient to be $<10 \text{ Mm}^{-1}$ at both 370 and 880 nm (Fig. 27). The comparison of the absorption coefficient profiles from GARRLiC/GRASP and the surface and airborne in situ measurements did not show a good agreement at both wavelengths (Fig. 27). Even more so, the profile shapes were also different for the GARRLiC/GRASP and the airborne in situ measurements.

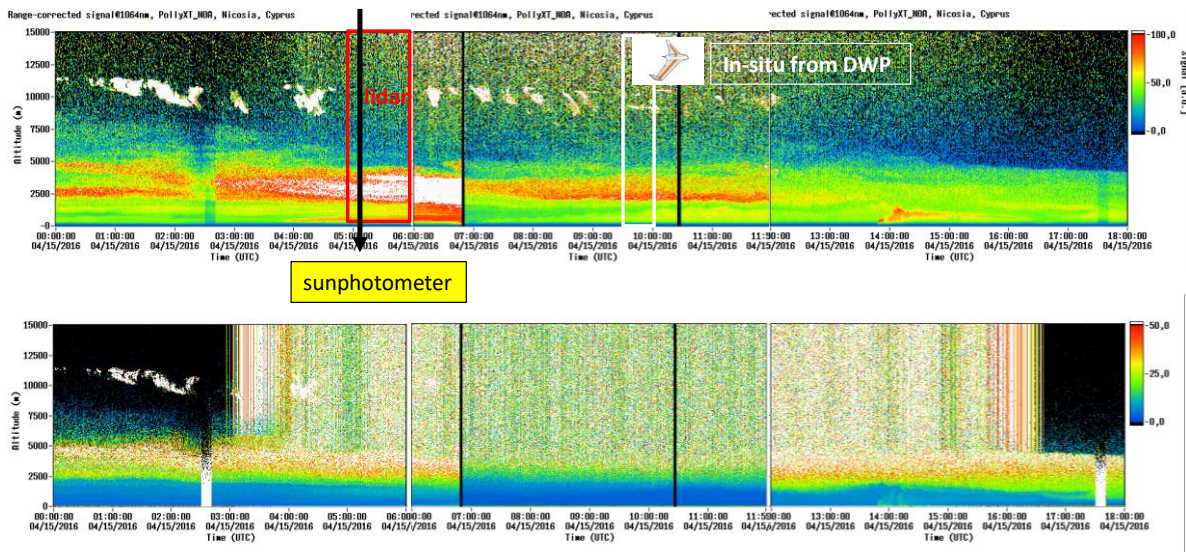


Figure 26: Top: Lidar range-corrected backscattered signal at 1064 nm, bottom: Cross/Total backscattered signal at 532 nm, on 15 April, 2016, during the JRA1 Cyprus campaign. The red box denotes the lidar measurements used for the absorption coefficient profile retrieval with the GARRLiC/GRASP algorithm at 5:00-6:00 UTC, the black line denotes the sun-photometer measurements at 5:06 UTC and the white box denotes the time range (9:27-9:55 UTC) of the in situ DWP measurements acquired with the Cyl UAV.

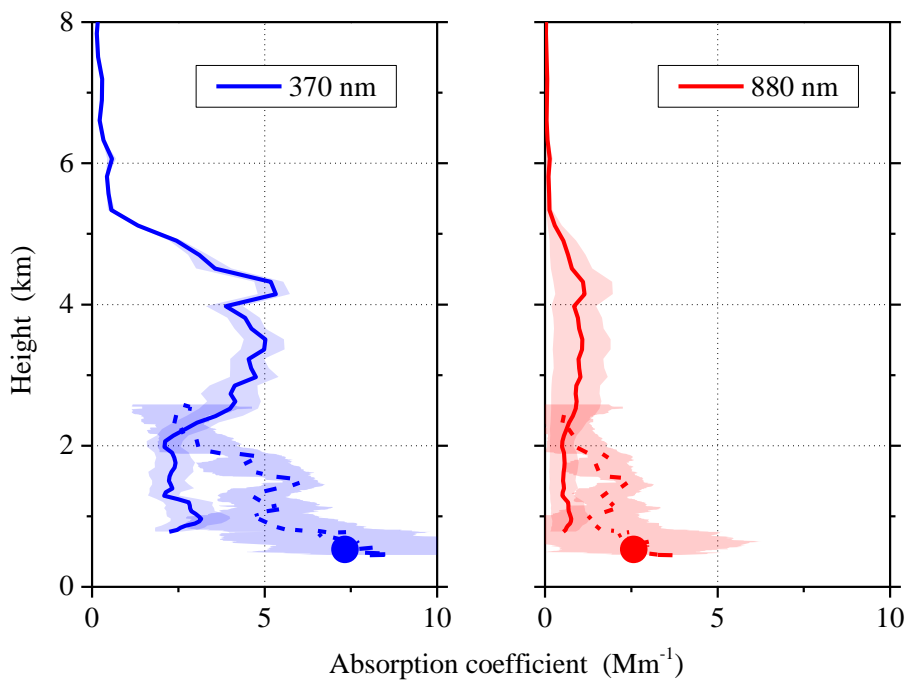


Figure 27. Absorption coefficient at 370 nm (left) and 880 nm (right) from GARRLiC/GRASP (solid colored lines) at 5:00-6:00 UTC, along with airborne measurements (dashed colored lines) from the DWP micro-Aethalometer onboard the Cyl UAV at 9:27-9:55 UTC, and surface in situ measurements (circles), on April 15, 2016.

Absorption profiles on 21/4/2016

On 21 April 2016 the dust episode was more intense, with AOD at 440 nm of 0.35 (Fig. 28). The airborne in situ measurements were conducted under cloudy conditions at 5:41-6:17 UTC, during which we could not perform the GARRLiC/GRASP retrieval. Instead we used lidar and sunphotometer measurements later in the day (at 12:00-13:30 UTC and 12:56 UTC, respectively). The dust plume showed variations throughout the day (Fig. 28), thus the comparison of non-collocated remote sensing and in situ measurements was not optimum.

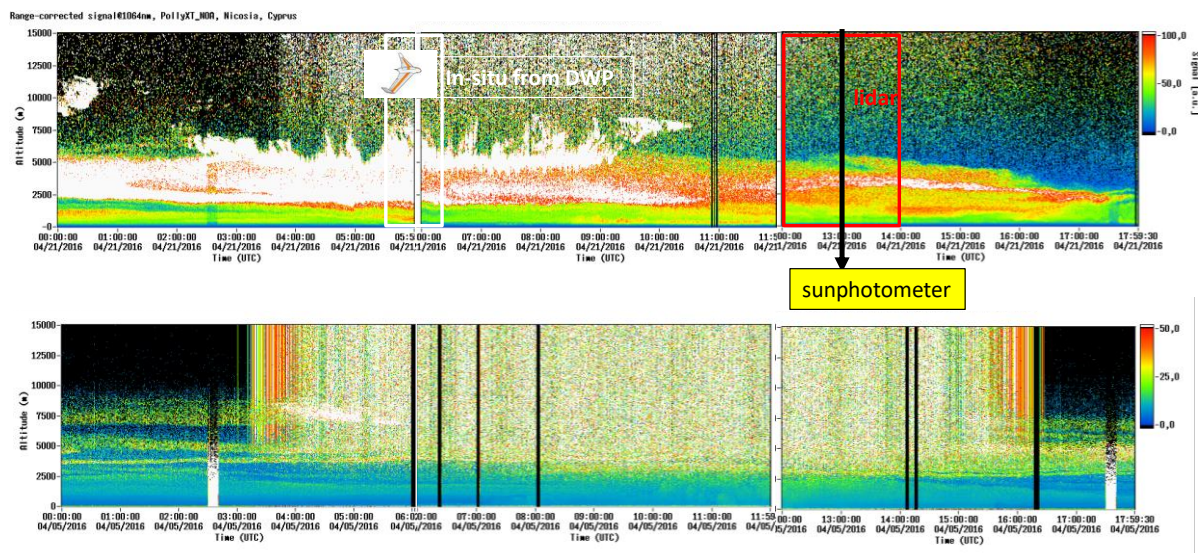


Figure 28: Top: Lidar range-corrected backscattered signal at 1064 nm, bottom: Cross/Total backscattered signal at 532 nm, on 21 April, 2016, during the JRA1 Cyprus campaign. The red box denotes the lidar measurements used for the absorption coefficient profile retrieval with the GARRLiC/GRASP algorithm at 12:00-13:30 UTC, the black line denotes the sun-photometer measurements at 12:56 UTC and the white box denotes the time range (5:41-6:17 UTC) of the in situ DWP measurements acquired with the Cyl UAV.

The particles were not strongly absorbing, with the absorption coefficient to be $<10 \text{ Mm}^{-1}$ at both 370 and 880 nm (Fig. 29). The absorption coefficient profiles from GARRLiC/GRASP, the surface and airborne in situ measurements agreed very well, within their uncertainties (Fig. 29).

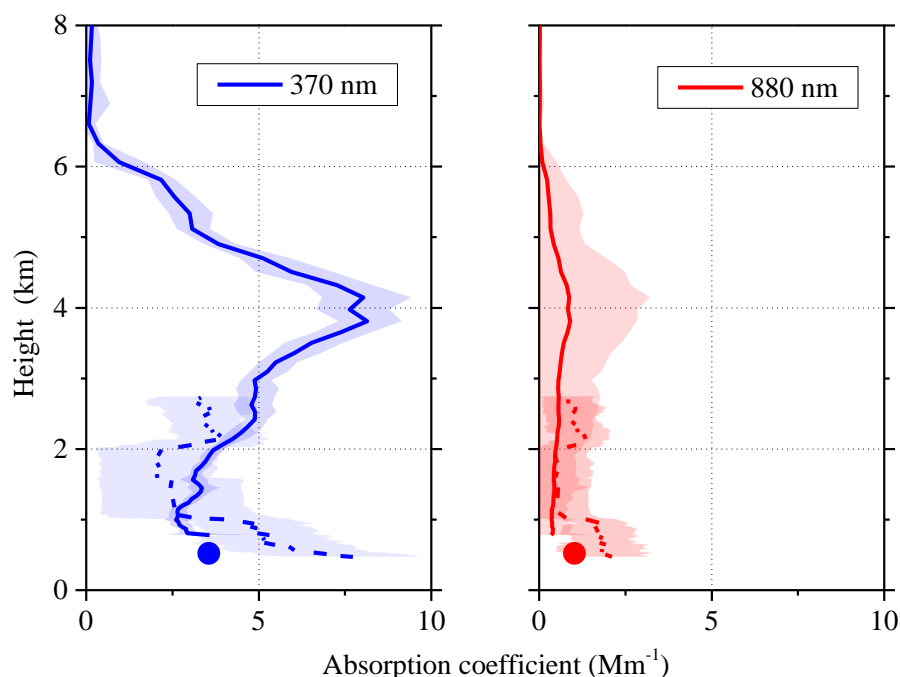


Figure 29. Absorption coefficient at 370 nm (left) and 880 nm (right) from GARRLiC/GRASP (solid colored lines) at 12:00-13:30 UTC, along with airborne measurements (dashed colored lines) from the DWP micro-Aethalometer onboard the Cyl UAV at 5:41-6:17 UTC, and surface in situ measurements (circles), on April 21, 2016.

3.4. SLOPE I AND II CAMPAIGNS AT GRANADA

SLOPE (Sierra Nevada Lidar AerOsol Profiling Experiment) campaigns was intended to determine the vertical structure of the aerosol by remote sensing instruments and test the various retrieval schemes for obtaining microphysical and optical properties. The main objective of this campaign was to perform a closure study by comparing remote sensing system retrievals of atmospheric aerosol properties, using remote systems operating at the Andalusian Institute of Earth System Research (IISTA-CEAMA) and in-situ measurements operating at different altitudes in the Northern slope of Sierra Nevada, around 20 km away from IISTA-CEAMA (Bedoya-Velázquez et al., 2018; Román et al., 2018). SLOPE I and II campaigns combined active and passive remote sensing measurements with in situ measurements, at several levels in the northern slope of Sierra Nevada. Furthermore, several flights with an instrumented plane provided aerosol vertical profiling. Different retrievals schemes were applied to the remote sensing data, to get aerosol microphysical profiles that were checked with the in situ information. Special care was paid to night-time remote sensing retrievals, combining multispectral Raman lidar with lunar and star/photometer and sky-cameras. Simultaneous operation of lunar and star photometer during several lunar cycles were used for testing and comparing both methodologies. Active remote and passive remote sensing instruments were operated at the Andalusian Institute for Earth System Research (IISTA-CEAMA) in Granada, UGR, (37.16°N, 3.61°W, 680 m a.s.l.), Spain. In situ instrumentation and a lunar/sun CIMEL radiometer were operated at the Albergue Universitario, SNS, (37.09°N, 3.39°W, 2500 m a.s.l.). Airborne in-situ measurements were collected in the vertical column over the valley station.

Measurements

Surface In-situ measurements

In-situ sampling at surface level took place in the Albergue Universitario of the University of Granada, located in Sierra Nevada (37.09°N, 3.39°W, 2500 m a.s.l.), SNS station. The surrounding mountains had elevations of approx. 3400 m, extending to distances of 20 km from the sampling location. All instruments were located in a room below the flat roof of the building. A pipe with a diameter of 10 cm extended 2.1 m above the roof and into the laboratory. A blower maintained a flow of 0.00167 m³s⁻¹; all instruments used in the SLOPE I and II campaigns (Integrating Nephelometer, Aerodynamic Particle Sizer (APS), Multi Angle Absorption Photometer (MAAP), Scanning Mobility Particle Spectrometer (SMPS), Aethalometer (A33)), and the polar nephelometer) sampled from this pipe. The residence time of the air in the pipe was 0.6 s. Losses in the pipe can be considered negligible. Aerosol absorption was monitored using an Aethalometer (AE33 model, Magee Scientific, Aerosol d.o.o.), and a Multi Angle Absorption Photometer (MAAP, Thermo) in combination with a TSI nephelometer (Model 3563) that measured total and backward scattering. Size distribution was measured by an OPC (Grimm model 1.109), a Aerodynamic Particle Sizer (APS, TSI 3321) spectrometer and a Scanning Mobility Particle Sizer (SMPS, TSI 3938) spectrometer. Additionally, during the second half of June 2016 (SLOPE I) the submicron chemical composition of non-refractory submicrometer particles was monitored in near-real time using an Aerodyne Aerosol Chemical Speciation Monitor (ACSM, Aerodyne Research Inc.).

Airborne In-situ measurements

A PARTENAVIA P68 collected vertical profiles of aerosol particles. The plane was equipped with an isokinetic isoaxial inlet with 2 flow splitter that divided the sampled air among the instruments. The plane was equipped with an Integrating Nephelometer (Aurora 3000, Ecothec), an aethalometer (AVIO AE33, Aerosol d.o.o.), an aerosol size spectrometer (SKY-OPC, GRIMM) and a water based particle counter (CPC, TSI 3787) together with some other meteorological and positioning instruments (Vaisala DMT (dew point temp.); Rotronic sensor (RH and T), GPS and Altimeter).

Several ascending vertical spiral profiles were performed over UGR station (Fig 30), covering the heights from ~1000 m asl to the top altitude around 4750 m asl. Table 3 includes information on the flights during SLOPE I and II campaigns.

Table 3. Instrumented flights during SLOPE I and II.

SLOPE I	SLOPE II
RF #1: 15 June 2016 15:15 – 18:00 UTC	RF #1: 21 June 2017 16:00 – 18:00 UTC
RF #2: 17 June 2016 12:50 – 15:00 UTC	RF #2: 23 June 2017 13:00 – 14:45 UTC
RF #3: 18 June 2016 08:00 – 10:30 UTC	RF #3: 24 June 2017 08:30 – 10:40 UTC



Figure 30. SLOPE campaigns scheme.

Remote sensing measurements

Intensive ground-based active and passive remote sensing measurements were acquired at IISTA-CEAMA. Active remote sensing was performed by MULHACEN (customized version of the multi-wavelength Raman lidar LR331D400- Raymetrics Inc.), a biaxial ground-based Raman lidar system. This system operates with a pulsed Nd:YAG laser, frequency doubled and tripled by Potassium Dideuterium Phosphate crystals, emitting at wavelengths of 355, 532 and 1064 nm with output energies per pulse of 60, 65 and 110 mJ, respectively. MULHACEN operates with three elastic channels: 355, 532 (parallel and perpendicular polarization) and 1064 nm and three Raman-shifted channels: 387 (from N₂), 408 (from H₂O) and 607 nm (from N₂). MULHACEN's overlap is complete at 90% between 520 and 820 m a.g.l. for all the wavelengths, reaching full overlap around 1220 m a.g.l.

Daytime sky radiance and AOD were measured by the sun-sky-lunar Cimel CE318-T photometer (Cimel Electronique). The optical sensor head has two detectors which cover the spectrum from 340 to 1064 nm. The CE318-T also performed direct lunar irradiance measurements, which were used to obtain AOD at night at 440, 500, 675, 870, 1020 and 1640 nm following the method proposed by Barreto et al. (2018).

Additional remote sensing instruments operated from UGR station included a Microwave Radiometer MWR (RPG-HATPRO G2, Radiometer physics GmbH), a Doppler lidar system (HALO photonics Stream Line) and a ceilometer (CHM-15k Nimbus, Lufft). The CHM-15k Nimbus ceilometer (Lufft) that is part of the Iberian Ceilometer Network ICENET (Cazorla et al., 2017) operates continuously emitting laser pulses at 1064 nm (a pulsed Nd:YAG laser) and measuring the backscattered signal by the atmosphere at different heights (up to 15360 m a.g.l.) with 15 m resolution. According to the overlap function provided by the manufacturer, the overlap is 90% complete between 555 and 885 m a.g.l.

SLOPE I

During the period of instrumented flights of SLOPE I the aerosol load is relatively load and the vertical profiling (Figure 31) reveals the presence of boundary layer aerosols during the flights.

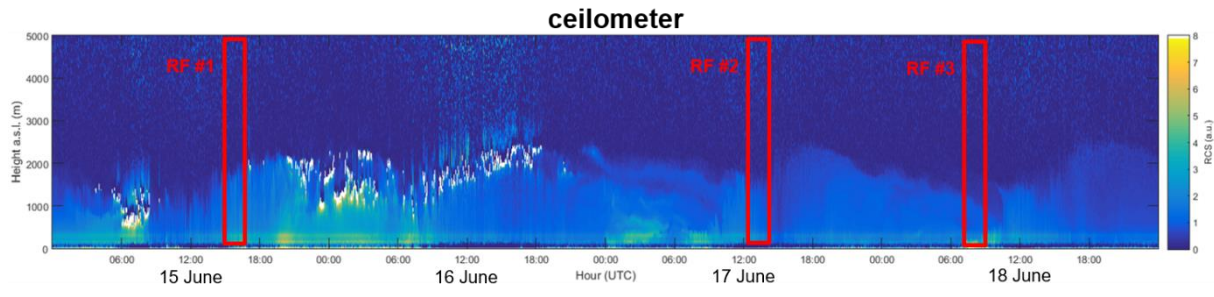
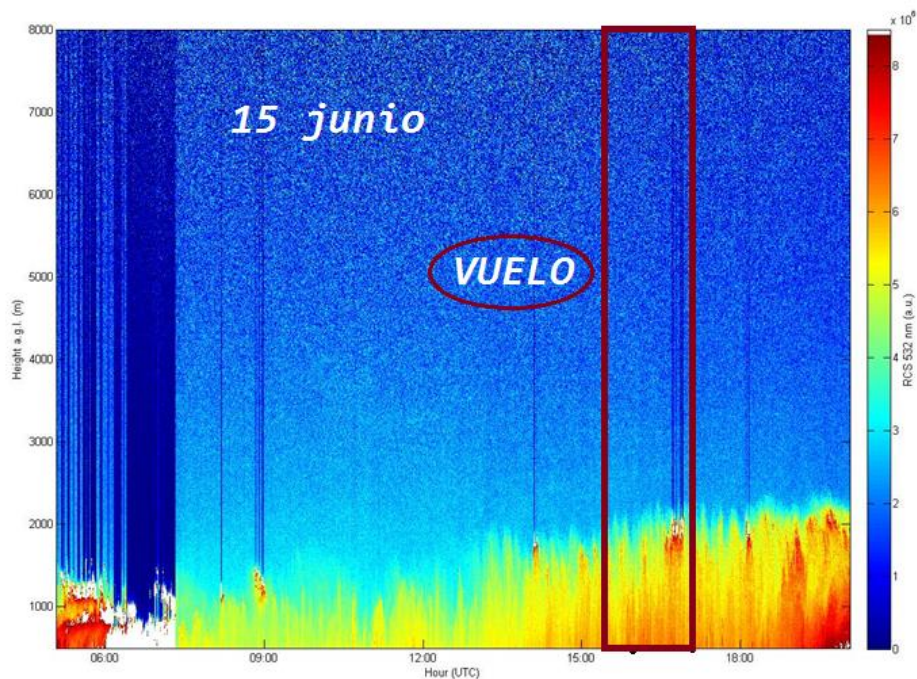


Figure 31. Vertical range-corrected backscattered signal at 1064 nm provided by the ceilometer during SLOPE I instrumented flights. The red box denotes the lidar measurements used for retrievals with GARRLiC/GRASP algorithm in coincidence with the flight profiling.

Absorption profiles on 15/06/2016

On 15 June 2016 MULHACEN lidar identifies the growth of the PBL and the absence of lofted aerosol layers (Fig 32). Several vertical flights monitored the vertical column over the valley station from 15:15 till 18:00 UTC.



op.

Figure 32. Lidar range-corrected backscattered signal at 532 nm, on 15 June 2016, during SLOPE JRA1 campaign at Granada. The red box denotes the lidar measurements used for the absorption coefficient profile retrieval with GARRLiC/GRASP algorithm in coincidence with the flight profiling.

Flights during SLOPE I measured rather clean conditions that represent a challenge for GRALiC/GRASP retrievals. The comparison of the absorption coefficient and SSA profiles from GARRLiC/GRASP and the airborne in situ measurements are shown in Fig. 33. The discrepancies among the absorption coefficient and SSA profiles measured by the airborne in situ instruments during the flights and retrieved by GARRLiC/GRASP were within the uncertainties associated to the corresponding retrievals. The IISTA-CEAMA measurements, denoted by the black dot at the valley were representative of the urban

atmosphere and differ from the lowest values in the vertical profiles level. The measurements at the mountain site presented good agreement with the vertical profiles in terms of the SSA, thus indicating that the airborne in situ and the surface in situ instruments at the mountain site observed the same kind of aerosol.

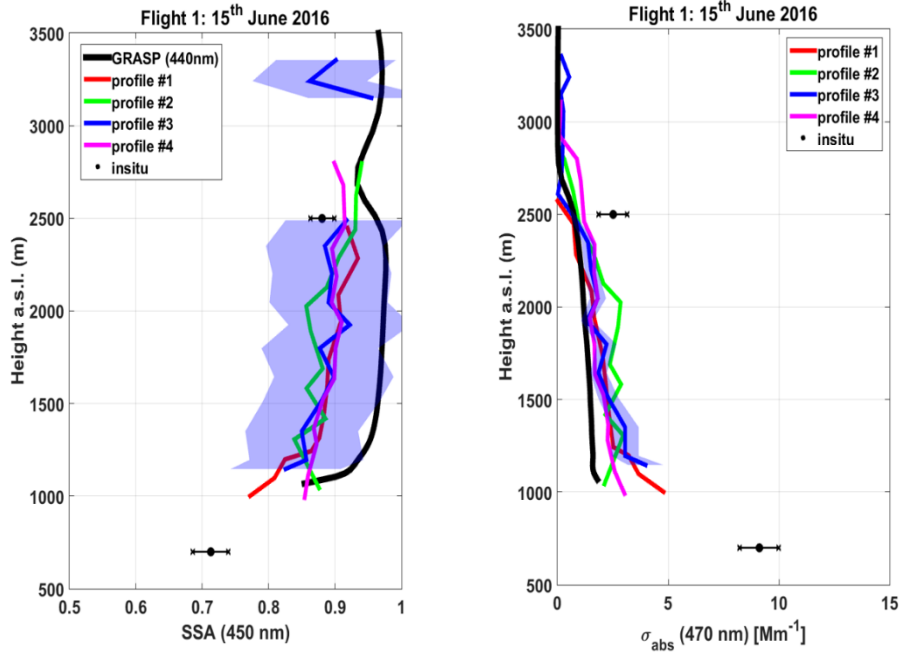


Figure 33. SSA at 450 nm (left) and absorption coefficient at 470 nm (right). The black lines correspond to the vertical profiles retrieved by GARLIC/GRASP algorithm while the solid colored lines correspond to the airborne in situ profiles retrieved from the different flights. The grey shadows denote the uncertainties associate to the retrievals. The black dots denote the in-situ measurements at the valley and mountain sites.

SLOPE II

During the period of instrumented flights of SLOPE II mineral dust have been detected (Figure 34). According to the surface in-situ measurements at UGR and SNS stations the dust affected only the mountain site in coincidence with the 24th June flight (RF #3) being negligible the effect over the valley station.

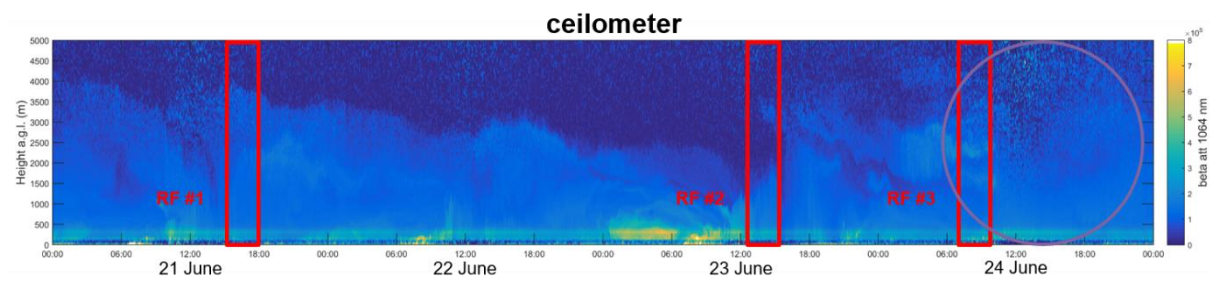


Figure 34. Vertical range-corrected backscattered signal at 1064 nm provided by the ceilometer during SLOPE II instrumented flights. The red box denotes the lidar measurements used for retrievals with GARRLiC/GRASP algorithm in coincidence with the flight profiling.

Absorption profiles on 23-24/06/2017

Figure 35 shows the absorption coefficient profiles retrieved by the instrumented flights and the use of GARRLiC/GRASP on 23-24 June. The agreement between both techniques is remarkable over 2000 m a.s.l., while the deviation is evident below this altitude. As in SLOPE I there are discrepancies between the SNS and airborne in-situ measurements at 2500 m a.s.l.

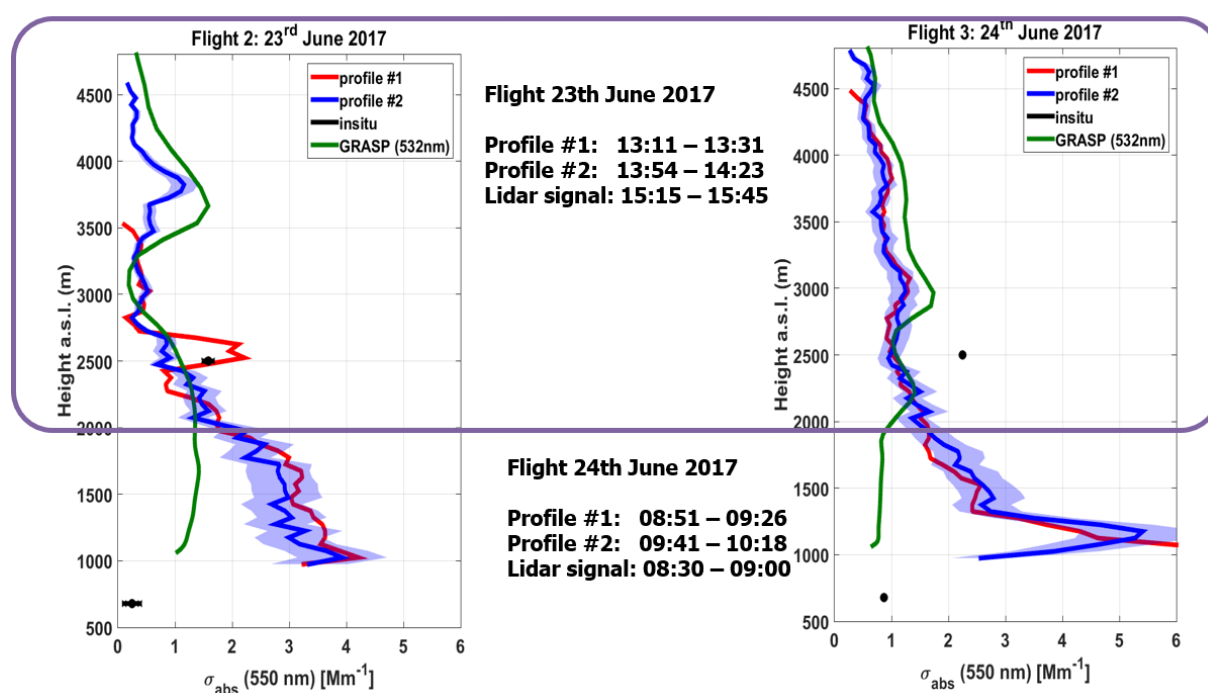


Figure 35. Absorption coefficient at 500 nm for 23/06/2017 (left) and 24/06/2017 (right). The green lines correspond to the vertical profiles retrieved by GARRLiC/GRASP algorithm while the blue and red lines correspond to the airborne in situ profiles retrieved from the different flights. The grey shadows denote the uncertainties associate to the retrievals. The black dots denote the in-situ measurements at the valley and mountain sites.

4 STANDARD OPERATING PROCEDURES –RECOMMENDATIONS FOR THE FUTURE

The ACTRIS-2 JRA1 campaigns highlighted the potential of the combined lidar/sunphotometer retrievals in deriving the aerosol absorption coefficient and SSA atmospheric profiles. **The closure between the**

remote sensing retrievals and the in situ measurements showed that their retrievals are reliable for sufficient aerosol load, with AOD at 440 nm larger than $\sim 0.3-0.4$.

A complete list of standard operating procedures is not possible at this point, since the following are missing. We provide them here as recommendations which can also be used in future efforts that include combined in situ and remote sensing measurements (e.g. ACTRIS PPP):

1. Need to quantify the airborne in-situ absorption coefficient uncertainties, so as the comparison with the remote sensing retrievals provide more conclusive results (action currently being conducted in a scientific paper to be submitted in Atmos. Meas. Tech.).
2. Acquire and utilize the near-range lidar measurements, so as to achieve the derivation of absorption coefficient and SSA profiles close to the ground. This is essential for cases where most of the aerosol load resides below 1 km. The utilization of the near-range measurements in the GARRLiC/GRASP retrieval is not trivial, since it requires gluing of the near-range with far-range lidar backscatter signals.
3. In case of dust absorption, in-situ monitoring of the coarse mode absorption is needed. We are not aware of a relevant light-weight instrument that can be carried from UAVs or tethered balloons. The ACTOS platform provides the capability of filter sampling, but it hasn't been used in dust-loaded regions during the ACTRIS-2 JRA1 campaigns. Nevertheless, coarse mode absorption in the vertical column can be extrapolated with ground-based measurements of dust mass absorption efficiency and dust concentration measurements performed by UAV.
4. Maximize the collocated in-situ/remote sensing measurements, possibly by extending the campaign duration and performing night-time flights, in order to achieve a large number of useful cases for every campaign. This is essential for the compilation of the representative aerosol absorption model for climate studies.
5. Since the in-situ measurements dry the aerosol sampled whereas the remote sensing retrievals provide the aerosol properties in ambient conditions we need to avoid measuring in high humidity conditions. This is usually the case in the free troposphere. The other solution is to model the hygroscopic growth of the particles. This may be possible with the new set of aerosol sensors currently developed by NOAA (Boulder, CO) and tested onboard Cyl UAVs.
6. Perform night-time GARRLiC/GRASP and night-time lidar stand-alone retrievals. Organize night-time in-situ measurements with UAV/tethered balloon/helicopter flights for direct comparison with the remote sensing retrievals (need authorization from the civil aviation authorities).
7. Organize the future campaigns during periods of high aerosol loads, as these possibly provided from climatological data of the region. For the combined lidar/sun/lunar photometer approach we need to avoid the winter months if possible, to achieve cloud-free days.

5 REFERENCES

- Altstädter, B., A. Platis, B. Wehner, A. Scholtz, N. Wildmann, M. Hermann, R. Käthner, H. Baars, J. Bange and A. Lampert, ALADINA – an unmanned research aircraft for observing vertical and horizontal distributions of ultrafine particles within the atmospheric boundary layer, *Atmospheric Measurement Techniques (AMT)*, 8, 1627-1639, 2015.
- Barreto, Á., Cuevas, E., Granados-Muñoz, M. J., Alados-Arboledas, L., Romero, P. M., Gröbner, J., Kouremeti, N., Almansa, A. F., Stone, T., Toledano, C., Román, R., Sorokin, M., Holben, B., Canini, M., and Yela, M. The new sun-sky-lunar Cimel CE318-T multiband photometer – a comprehensive performance evaluation, *Atmos. Meas. Tech.*, 9, 631-654, 2016.
- Böckmann, C.: Hybrid regularization method for the ill-posed inversion of multiwavelength lidar data to determine aerosol size distributions, *Appl. Optics*, 40, 2001.
- Collaud Coen et al., *Atmos. Meas. Tech.* 3, 457-474, 2010
- Corbin, J. C., Müller, Th., Wehner, B., Tuch, Th., Bukowiecki, N., Baltensperger, U., and Gysel, M.: Evaluation of 3 CAPS PM_{2.5} monitors: aerosol absorption and single-scattering albedo measurements at a remote European site. Presented at the European Aerosol Conference 2016 in Tours, France.
- Dubovik, O., and M. D. King, 2000: A flexible inversion algorithm for retrieval of aerosol optical properties from sun and sky radiance measurements, *J. Geophys. Res.*, 105, 20,673 – 20,696.
- Engelmann, R., T. Kanitz, H. Baars, B. Heese, D. Althausen, A. Skupin, U. Wandinger, M. Komppula, I.S.Stachlewska, V. Amiridis, E. Marinou, I. Mattis, H. Linné and A. Ansmann, The automated multiwavelength Raman polarization and water-vaporlidar PollyXT: The neXT generation, *Atmos. Meas. Tech.*, 9(4), 1767-1784, 2016.
- Ferrero, L., Mocnik, G., Ferrini, B. S., Perrone, M. G., Sangiorgi, G. and Bolzacchini, E.: Vertical profiles of aerosol absorption coefficient from micro-Aethalometer data and Mie calculation over Milan, *Sci. Total Environ.*, 409(14), 2824–2837, doi:10.1016/j.scitotenv.2011.04.022, 2011.
- Kebabian et al., *Rev. Sci. Instruments* 78, 2007.
- Lopatin, A., et al.: Enhancement of aerosol characterization using synergy of lidar and sun-photometer coincident observations: the GARRLiC algorithm, *Atmos. Meas. Tech.*, 6, 2065-2088, doi:10.5194/amt-6-2065-2013, 2013.
- Mamali, D., Marinou, E., Sciare, J., Pikridas, M., Kokkalis, P., Kottas, M., Binietoglou, I., Tsekeri, A., Keleshis, C., Engelmann, R., Baars, H., Ansmann, A., Amiridis, V., Russchenberg, H., and Biskos, G.: Vertical profiles of aerosol mass concentration derived by unmanned airborne in situ and remote sensing instruments during dust events, *Atmos. Meas. Tech.*, 11, 2897-2910, <https://doi.org/10.5194/amt-11-2897-2018>, 2018.
- Müller, D., et al.: Comprehensive particle characterization from three-wavelength Raman-lidar observations, *Appl. Opt.*, 40, 4863–4869, 2001.
- Onasch et al., *Aerosol Sci. Technol.* 49, 267-297, 2015.
- Sandradewi, J., Prevot, A. S. H., Szidat, S., Perron, N., Alfarra, M. R., Lanz, V. A., Weingartner, E., and Baltensperger, U.: Using aerosol light absorption measurements for the quantitative determination of wood burning and traffic emission contributions to particulate matter, *Environ. Sci. Technol.*, 42, 3316–3323, 2008.
- Siebert, H., H. Franke, K. Lehmann, R. Maser, E. W. Saw, D. Schell, R. A. Shaw, M. Wendisch, Probing Finescale Dynamics and Microphysics of Clouds with Helicopter-Borne Measurements, *Bulletin of the American Meteorological Society*, 87(12), 1727–1738, 2006.
- Spindler, G., A. Grüner, K. Müller, S. Schlimper, H. Herrmann, Long-term size-segregated particle (PM₁₀, PM_{2.5}, PM₁) characterization study at Melpitz – influence of air mass inflow, weather conditions and season, *J. Atmos. Chem.*, 70, 165 - 195, 2013.
- Virkkula, A., Ahlquist, N. C., Covert, D. S., Arnott, W. P., Sheridan, P. J., Quinn, P. K., and Coffman, D. J.: Modification, Calibration and a Field Test of an Instrument for Measuring Light Absorption by Particles. *Aerosol Sci. Technol.* 39:68–83, 2005.

Virkkula, A.: Correction of the Calibration of the 3-wavelength Particle Soot Absorption Photometer (3PSAP), *Aerosol Sci and Technol*, 44, 706, 2010.

Weingartner, E., Saathoff, H., Schnaiter, M., Streit, N., Bitnar, B., and Baltensperger, U.: Absorption of light by soot particles: determination of the absorption coefficient by means of aethalometers, *J. Aerosol Sci.*, 34, 1445-1463, doi:10.1016/S0021-8502(03)00359-8, 2003.

Wildmann, N., Hofsäß, M., Weimer, F., Joos, A., and Bange, J.: MASC—a small remotely piloted aircraft (RPA) for wind energy research, *Adv. Sci. Res.*, 11, 55–61, doi:10.5194/asr-11-55-2014, 2014.